

A Technology Pathway for Airbreathing, Combined-Cycle, Horizontal Space Launch Through SR-71 Based Trajectory Modeling

Kurt J. Kloesel*, Nalin A. Ratnayake† and Casie M. Clark‡

NASA Dryden Flight Research Center, Edwards AFB, California, 93523

Access to space is in the early stages of commercialization. Private enterprises have been making headway into low-Earth orbit launch systems for small-weight-class payloads of approximately 1,000 lb. These modest gains have emboldened the launch industry, which is now poised to move into the middle-weight class (approximately 5000 lb). The majority of these commercially successful systems are based on relatively straightforward two-stage, liquid propellant rocket technology developed by the United States Government 40 years ago, accompanied by many technology improvements. Configurations that incorporate airbreathing, reusable carrier vehicles for the first launch stage are the next paradigm in developing game-changing access-to-space technologies. While many conceptual designs exist, technological advancement in key areas such as combined-cycle engines is predicated upon successful flight research. In this study, airbreathing access-to-space is addressed from the specific perspective of bringing combined-cycle engine technology to flight research and the next level of readiness. The engines considered are based on or extrapolated from known performance parameters of rocket-based combined cycle (the Marquardt Corporation ejector ramjet) and turbine-based combined cycle (the Pratt & Whitney J-58 engine used in the Lockheed SR-71 Blackbird). Validated engine models are coupled with trajectory simulation and analysis in multiple software tools to explore viable launch scenarios using a hypothetical aerospaceplane platform conforming to the aerodynamic model of the SR-71. This aerodynamic model is augmented to simulate an attached orbital insertion vehicle by including the drag increment of the Linear Aerospike SR-71 Experiment. Finally, recommendations are made in support of advocacy of successful adoption of combined-cycle engine systems for space access. The recommended pathway is founded on the principle of concentrating on the technologies of specific interest, while reducing risk and complexity in every other aspect of such a program. In this sense, leaping to fully-integrated conceptual systems is rejected in favor of focused flight research in key technologies.

Nomenclature

γ	Flight path angle, deg
Φ_r	Primary rocket equivalence ratio
I_{sp}	Specific impulse, lbf-s/lbm
DRACO	Demonstration of Rocket and Airbreathing Combined-cycle Operation
GECAT	Graphical Engine Cycle Analysis Tool
KEAS	Knots Equivalent Air Speed
LASRE	Linear Aerospike SR-71 Experiment
LEO	Low-Earth Orbit

*Aerospace Engineer, Aerodynamics and Propulsion Branch, M/S 4840B, AIAA Member.

†Aerospace Engineer, Aerodynamics and Propulsion Branch, M/S 4840B, AIAA Senior Member.

‡Motivating Undergraduates in Science and Technology (MUST) intern, Aerodynamics and Propulsion Branch, M/S 4840B, AIAA Student Member.

LOX Liquid Oxygen
NASA National Aeronautics and Space Administration
OTIS Optimal Trajectories by Implicit Simulation
POST Program to Optimize Simulated Trajectories
RBCC Rocket-Based Combined-Cycle
RP Rocket Propellant (kerosene)
SPAD Space Propulsion Analysis and Design
STP Standard Temperature and Pressure
TBCC Turbine-Based Combined Cycle

I. Introduction

Few subjects in the arena of technological development over the last sixty years have produced more innovative and varied ideas for implementation than that of how we human beings may most effectively leave the planet of our origin. Yet, despite the vast number of potential concepts, access-to-space has in practice remained without a paradigm shift since the days of Wernher von Braun. The conventional liquid-fuel rocket engine has undergone many technological advances over the past few decades, but the fundamental mode of operation remains essentially unchanged since that of the earliest examples of modern liquid-fueled rocketry. Present policy on space exploration and technology development is now amenable to the consideration of alternative access-to-space technologies. Air carrier or horizontal launch systems, electromagnetic rail launch, and other such concepts now have the potential to receive greater attention, as well as research and development investment.

Since the beginnings of the space program, the development of new vehicles has always relied on aeronautics-based technologies to advance to each new paradigm in space flight. The first era of large rocketry up through the Apollo program drew heavily on early work by von Braun, Hermann Oberth, and others in supersonic aerodynamics, stability and control systems, gas dynamics, et cetera. The next era, that of the Space Shuttle, required development of the more advanced reentry aerodynamics associated with lifting bodies, as well as advances in hypersonic gas dynamics and other fields. The present dawning of the third age of human space flight will similarly require investment in aeronautics and flight research in order to be successful. The analysis tools and much of the technology for these systems largely already exist.

Combined-cycle engines can utilize multiple propulsion cycles in the same physical system. Their design, operation, and performance have long been the the subjects of engineering consideration. Airbreathing access-to-space, particularly involving the analysis of combined-cycle engine technology, has been discussed in numerous previous studies, such as those by Hueter;¹ Liu, Wang, and Cai² ; Daines³ ; and Chase.⁴ The two leading candidates for aerospace combined-cycle engine technology are rocket-based combined-cycle (RBCC) and turbine-based combined-cycle (TBCC). Paper studies, computational analysis, and, in many instances, small- or full-scale ground-test data exist for a number of proposed combined-cycle engine systems. What is lacking in the combined-cycle engine community is access to relevant flight data to validate these models, and a pathway that links present modeling efforts to specific flight research objectives and assets. This paper provides:

- Engine modeling of a representative RBCC using the Graphical Engine Cycle Analysis Tool (GECAT), as well as tabular models of a TBCC based on historical data.
- Validation of these engine models against physical test data; in the case of the RBCC, the Marquardt Corporation ejector ramjet,⁵ and in the case of the TBCC, a tabular representation of the Lockheed (now Lockheed Martin, Bethesda, Maryland) SR-71 engine constructed around the Pratt & Whitney (Bloomfield, Connecticut) J-58 engine core.⁶
- Incorporation of the engine models into ascent trajectory optimization and performance analysis through the Program to Optimize Simulated Trajectories II (POST II)⁷ and Optimal Trajectories by Implicit Simulation (OTIS),⁸ using an aerodynamic model borrowed from the Lockheed SR-71 aircraft.
- A proposed pathway for research and technology development that will enable combined-cycle engine technology to advance to flight research in an expeditious manner.

It is not the intent of this study to design an integrated spacecraft or perform a figure-of-merit comparison between RBCC and TBCC technologies, but rather to explore the extent to which present (or even legacy) systems may be used to bring either of these engine technologies to flight research as efficiently as possible. To this end, independent researchers studied the TBCC and RBCC modes of airbreathing access-to-space; no attempt was made to quantitatively assess an overall advantage of one over the other. The results of both sub-studies are presented.

A. Rocket-Based Combined Cycle Engines: Background

Rocket-based combined-cycle engines are syntheses of rocket and airbreathing propulsion systems that can operate in “ejector” (ducted rocket), ramjet, scramjet, and pure rocket modes.⁹ During operation in the ejector mode (suitable for ground launch), the thrust from the rocket engine is augmented by the entrained air from the ejector action of the rocket plumes flowing inside the airbreathing flowpath. The remaining three modes, listed in the order of their usually-designed phase of operation, are more well-known engine concepts, and are assumed to be largely self-explanatory. Rocket-based combined-cycle engines could be the first or intermediate stage in a multistage system for space launch.

An RBCC-type engine operates in one or more airbreathing modes at altitudes low enough to provide adequate mass ingestion to use oxygen from the atmosphere, and then switches to pure rocket operation at higher altitudes and in space flight. The airbreathing mode allows the craft to avoid carrying the mass of the oxidizer that is required for ascent through the lower altitudes, and thus in theory realizes a significant propellant weight savings (and associated increased payload fraction) over pure rockets. The savings are estimated to be possibly as high as a factor of five to ten,¹⁰ although these claims are generally the result of modeling studies and are unverified by substantial flight data as of yet. The large savings in propellant mass are, however, counteracted by increased system dry mass.

Rocket-based combined-cycle development efforts, at least in a conceptual sense, have been ongoing since the 1940s. Naturally, a comprehensive history of RBCC development over the last half century is not possible here; however, selected studies from the 1990s to the present are given attention.

In the mid-1990s, ground tests of an ejector scramjet testbed were performed at the National Aeronautics and Space Administration (NASA) Lewis (now Glenn) Research Center (Cleveland, Ohio) Plumbrook Research Station in conjunction with Aerojet (Sacramento, California), the General Applied Science Laboratory, and the United States Air Force (USAF) HyTech program. Data from these tests were used to develop potential RBCC test trajectories in POST associated with the X-34 vehicle.¹¹ Further testing at Lewis of an RBCC-type engine in the Hypersonic Test Facility provided ground-test data for Mach 5 and Mach 6 and some validation of computational fluid dynamics flowpath modeling.¹² The NASA Glenn Research Center also led a program to design the GTX vehicle,¹³ which utilized three RBCC engines; several papers are available in the literature regarding this program.

The Highly Reusable Space Transportation study conducted by NASA from 1995-1997 looked at several advanced space launch systems for single- and two-stage-to-orbit systems, RBCC-powered systems being one of the many options considered. Mankins¹⁰ provides an overview of the trade studies and modeling efforts performed by the government as well as numerous academic institutions on RBCC technology (see in particular pages 8 through 10) on inlets, combustion, and performance. All of the studies mentioned were conceptual, lacking flight-data validation.

In 1999, the NASA Marshall Space Flight Center (MSFC) (Alabama) began leading an in-house program involving the NASA Stennis Space Center (SSC) (Mississippi) and the NASA Dryden Flight Research Center (Edwards, California) to develop, ground test, and eventually flight test an RBCC engine. This program was called the Demonstration of Rocket and Airbreathing Combined-cycle Operation (DRACO). The MSFC was to lead the development effort, SSC to provide ground-testing support, and DFRC to flight test the final article by 2005, according to internal documents and other publications.¹ The focus of this effort was the development of an RBCC engine that would use hydrocarbon-based fuel instead of liquid oxygen and liquid hydrogen (LOX/LH2) or the similar propellant combinations used in previous RBCC concepts. This in-house NASA RBCC engine, however, was not developed.

B. Turbine-Based Combined Cycle Engines: Background

Turbine-based combined cycle engines operate by using a gas turbine propulsion cycle which transitions to a ramjet cycle; they bypass the turbomachinery at high Mach numbers, where pressures, temperatures, and

flow velocities make such machinery impractical or redundant or both. Such a configuration by itself is not capable of orbital insertion because at some altitude the ramjet mode will lack the inlet mass flow to sustain thrust; however, TBCC engines hold strong promise for use with carrier vehicles or atmospheric ascent stages. Turbojet propulsion systems are generally limited to Mach 3 due to the rise in inlet temperature present at the compressor face; turbine engines are also in general more limited in altitude with respect to their ramjet counterparts as well. They provide more efficient operation, however, at lower altitudes and Mach numbers relative to ramjet-based engines.¹⁴ The limitation to lower Mach numbers and altitudes is not universal, especially if the ramjet mode is effective enough to compensate for the additional weight of the turbomachinery.

Turbine-based combined-cycle engines have seen actual flight time, a qualification which is not shared by RBCC engines. For example, the SR-71 J-58 engine is a turbine-based engine that operates in multiple cycles depending on the flight regime (with known cruise conditions of approximately Mach 3.2 at an altitude of 70,000 ft). Additionally, recent advanced hypersonic systems such as the Defense Advanced Research Projects Agency (DARPA) and USAF Force Application and Launch from the Continental United States (CONUS) (FALCON) Blackswift program have proposed using TBCC-class propulsion systems.¹⁵ The DARPA also studied the Responsive Access Small Cargo Affordable Launch (RASCAL) vehicle¹⁶ in the early 2000s, which, though it did not utilize an integrated combined-cycle engine in the purest sense, did make use of multiple engine cycles in the same launch system. As such, TBCC engines can likely be considered a more mature technology when compared to RBCC engines, but the latter are not far behind.

For most cases, at least some turbine operation will most likely be required for a significant portion of the trajectory in order to provide system power for the operation of the vehicle. The RBCC engine, by comparison, cannot directly supply on-board power; thus, an additional auxiliary power unit or power supply would likely be necessary for such systems.

C. The SR-71 Aerodynamic Model

From the perspective of flight researchers, there is no need to reinvent the wheel for systems that are not the primary subject of interest. Conceptual designs of new vehicles abound in the literature, and although they may hold substantial merit from a design perspective, in practicality the development of completely new vehicles (either for the orbital stage or the boost or carrier stage) is complex and expensive. Flight research inherently relies on a build-up approach. The pathway to full flight demonstration of such a launch vehicle must include appropriate time for the component technologies to individually undergo flight research and thus attain maturity.

The key technology advocated in this paper is that of combined-cycle engines. Thus, other aspects of the research vehicle, including the aerodynamic model, should utilize as much proven technology as possible. The Pratt & Whitney J-58 engine and its installed performance in the surrounding SR-71 propulsion system are known from abundant hours of flight research, testing, and service flight at NASA and with the USAF. Figure 1 shows the SR-71 in flight carrying the Linear Aerospike SR-71 Experiment (LASRE).

Simulation and optimization of potential ascent and launch trajectories requires an aerodynamic model.¹⁷ Following the philosophy of advancing to flight-testing rapidly and effectively, a known quantity is first taken as a baseline, using as many known and proven systems as possible without jeopardizing the advancement of the specific, innovative technology being studied (in this case, combined-cycle engines). The platform selected, based on its proven high-altitude, high-speed cruise capability and known load capacity, is the Lockheed SR-71.

In addition to altering the baseline aerodynamics, the attachment of a small launch vehicle to the back of a theoretical supersonic air carrier will alter the zero-lift drag characteristics. Two known mated tested configurations exist for the SR-71. The first is the MD-21 (mother-daughter) which was a structurally reinforced SR-71 with a mated D-21 drone capable of speeds in excess of Mach 3.0. The second is the LASRE, which was the object of a series of propulsion flight research performed at NASA DFRC in the 1990s.

The aerodynamic tables were obtained and input using Lockheed report¹⁸ SP-508. Wing area and weight was also obtained from this report. Thrust as a function of altitude, Mach number, and throttle setting was obtained from historical simulation runs to Mach 3.2 that were performed by NASA DFRC using the legacy Singer-Link simulator. The thrust information also included a break point between full military and afterburner settings.



Figure 1. The Lockheed SR-71 Blackbird in flight with the Linear Aerospike SR-71 Experiment (LASRE) attached.

Initial tests of the model were simulated using level flight at an altitude of 70,000 ft to determine if the cruise performance compared well with known data. Model level-cruise performance was found to be beyond 1000 nm, which was in the order of magnitude of the performance of the SR-71. The validation process then considered the fuel consumption performance during climb using the nominal climb profile described in the SR-71 flight manual.¹⁹ The profile consists of a constant dynamic pressure subsonic climb at 400 knots equivalent airspeed (KEAS), a transonic penetration dive, and a 450-KEAS constant dynamic pressure climb to the higher altitudes. Following this initial attempt, a more detailed validation case is shown against flight data from flight 46 of the SR-71 in Figure 2.

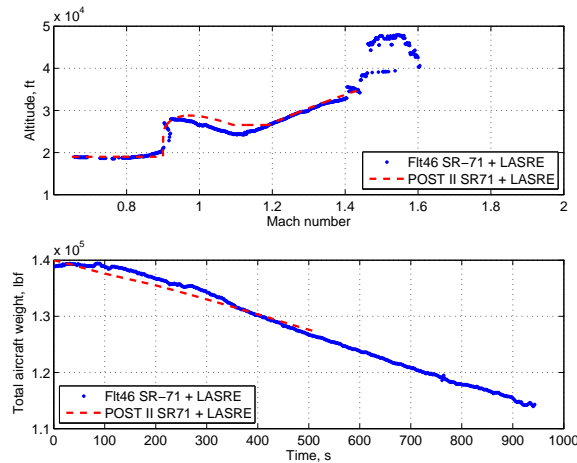


Figure 2. Aerodynamic model validation case in POST II compared to data from Flight 46 of the SR-71 with the LASRE.

The base SR-71 model was used for initial ascent simulations, and the LASRE drag increment was added using additional data from the SR-71 flight-test experiments. These data included Flight 46, which was used for the validation case. Note that an attached launch vehicle would impart a much larger drag increment than the LASRE; however, it is also probable that modern engine technology could deliver better performance than the legacy systems considered in this study. The specific nature of this improvement is

immaterial, as the objective of the paper is not to design a new conceptual system, but to demonstrate that combined-cycle engine technology can be brought to flight research even using a hypothetical carrier vehicle based on decades-old technology.

II. Engine Modeling

Two engine models were used for the trajectory simulations. The first was the Marquardt MA139-XAA ejector ramjet (an RBCC). The second was the Pratt & Whitney J-58 engine core used in the Lockheed SR-71 engine system (a TBCC).

A. The Marquardt Ejector Ramjet Models

In the late 1950s and through the 1960s, the Marquardt Corporation conducted research on combined-cycle engines with their groundbreaking study of 36 different combined-cycle engine models under NASA contract NAS7-3772 as well as several contracts for the United States Army, Navy, and Air Force. To the authors' knowledge, this remains the most comprehensive hardware testing and development program for ramjet and RBCC engine systems to date that is available in the literature.

1. Base Model Development and Validation

The base model engine chosen was the 1968 ejector ramjet engine designed and tested by the Marquardt Corporation and described by Odegaard.⁵ A subscale "boilerplate" engine was subjected to ground-testing for a number of different configurations; full-scale, flight-weight models were subjected to more limited testing. Because of the greater quantity of test data available, the subscale engine was used for model validation. The validated model was then scaled up and adjusted to match the performance of the full-scale MA139-XAA engine, which is a flight-weight ejector ramjet capable of 60,000 lbf sea-level static thrust.²⁰ Both the subscale and full-scale engines chosen use liquid oxygen and rocket propellant (LOX/RP) for the primary (rocket) combustors, and hydrocarbon fuel for the afterburner.

The subscale Marquardt ejector ramjet engine consists of an inlet, a primary rocket section, a mixer, a diffuser, an afterburner, and an exit nozzle. Contained within the primary rocket section are eight individual rocket units arranged in an annular ring. Incoming air and rocket combustion products combine in the mixing region, where the flow proceeds through the diffuser and into the afterburner. In the afterburner, additional fuel is added and the mixture is re-burned. The flow is then expelled through a convergent or convergent-divergent nozzle, depending on the test condition.

The subscale engine was ground-tested at sea level static, Mach 1, and Mach 1.9 in ejector mode; and at Mach 1.9 in pure ramjet mode. The subscale engine was built with variable geometry to test different size inlets, mixing regions, diffuser angles, and nozzle diameters. For sea level static testing, a bellmouth inlet and convergent nozzle were used. For testing at Mach 1, the bellmouth inlet was replaced with a normal shock inlet; for testing at Mach 1.9, the convergent nozzle was replaced with a convergent-divergent nozzle. The Mach 1 and Mach 1.9 flight conditions were tested at simulated altitudes of 9,400 ft and 40,000 ft, respectively.

The software program GECAT was used to model the subscale Marquardt ejector ramjet, for which ground-test data exist for model validation.

2. The Graphical Engine Cycle Analysis Tool Model of the Subscale Engine

The Graphical Engine Cycle Analysis Tool (GECAT) software program is a graphical front-end to the NASA Engine Performance Program (NEPP).²¹ The GECAT enables the user to select different components and construct a custom engine or to choose from a list of built-in models. The configuration chosen to model the ejector mode is a modified ducted rocket/ramjet hybrid that consists of an inlet, duct, gas generator, mixer, diffuser, reactants injection station, and a nozzle. As in the Marquardt engine, there is an airflow stream from the inlet and a fuel stream from the rockets mixed in the mixer, and the resulting mixture is then further combusted and expelled through the nozzle.

The gas generator was chosen to model the primary rocket section, as it allowed for the specification of propellants, fuel flow, and oxidizer flow, as well as the modeling of the combustion process. The afterburner was modeled with a reactants injection station instead of a combustion chamber because the combustion

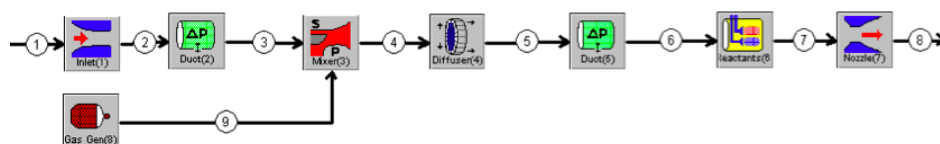
chamber component was found to be incompatible with the rest of the model setup. In simpler test models it was found that a reactants injection station yielded the same results as a combustion chamber, so it can be reasonably assumed that the two can be used interchangeably.

The reactants station allows for specification of fuel and oxidizer flow, and, in this case, is injecting the gas at a temperature high enough for theoretically instantaneous combustion. Ramjet-only mode was run with a separate GECAT model because much better results were obtained by having separate models for the ejector and ramjet modes. The default GECAT ramjet engine configuration was chosen, and modified by replacing the combustion chamber with a reactants station.

Modeling the engine proved to be a challenge because the Marquardt Corporation documentation did not supply all the needed variables. A model was thus developed by making reasonable estimates and comparing the results with the ground-test data for each case. The engine model chosen was the one that most closely approximated each test condition. Flowcharts of the GECAT models for the pure ramjet and the rocket ejector modes are shown in Figures 3(a) and 3(b), respectively.



(a) Pure ramjet operation flowchart.



(b) Ejector ramjet operation flowchart.

Figure 3. Flowchart of the Graphical Engine Cycle Analysis Tool model for the subscale Marquardt Corporation ejector ramjet.

3. Validation

The modeled thrust and specific fuel consumption for sea level static conditions are shown plotted against Marquardt Corporation test data in Figure 4. The multiple curves represent different primary (rocket) equivalence ratios, and the independent variable for all cases is the overall (rocket + combustor) equivalence ratio. Similar validation against data from a Mach 1.9 ground test of the Marquardt ejector ramjet is shown in Fig. 5.

The errors against test data for the GECAT RBCC model are summarized in Table 1. It is noted that the error in modeled thrust appears to be quite high for the sea-level static case at the lowest primary equivalence ratio (0.57). It is presumed that this error is due to the decreased accuracy of mixing and combustion dynamics the further away one moves from stoichiometric burning conditions.

Model error	Net thrust, percent	I_{sp} , percent
Static $\Phi_r = 0.95$	4.89	6.48
Static $\Phi_r = 0.77$	2.46	2.07
Static $\Phi_r = 0.57$	19.94	4.52
Mach 1.9 (ejector), $\Phi_r = 0.829$	2.09	6.58
Mach 1.9 (ramjet), $\Phi_r = 0.829$	5.25	8.47

Table 1. Average error versus Marquardt Corporation engine data for the Graphical Engine Cycle Analysis Tool rocket-based combined-cycle model at certain Mach numbers, configurations, and primary (rocket) equivalence ratios.

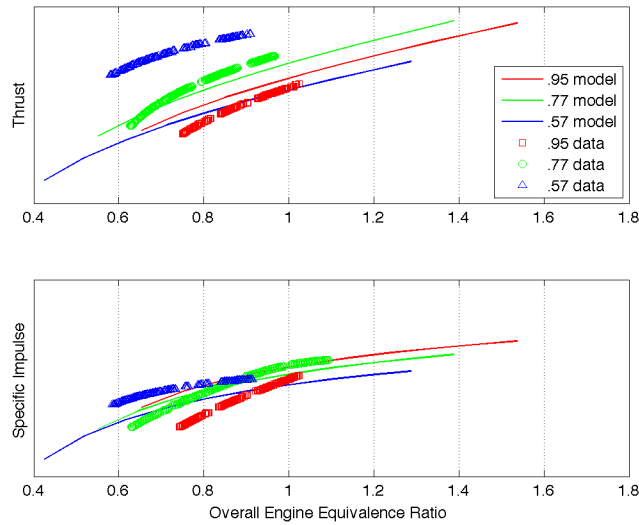


Figure 4. The Graphical Engine Cycle Analysis Tool rocket-based combined-cycle model estimates of sea level static thrust and specific impulse compared with the overall engine equivalence ratio, plotted against Marquardt Corporation test data.

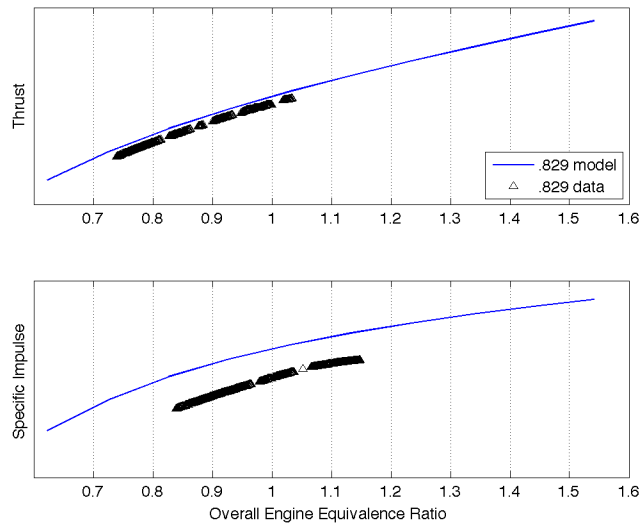


Figure 5. The Graphical Engine Cycle Analysis Tool rocket-based combined-cycle model estimates of sea level Mach 1.9 thrust and specific impulse compared with the overall engine equivalence ratio, plotted against Marquardt Corporation test data.

4. *The Full-Scale MA139-XAA Ejector Ramjet Engine*

The subscale engine model, having been validated against the ground-test data from the Marquardt Corporation, was then scaled up to match the performance characteristics of the MA139-XAA full-scale ejector ramjet as described by the Marquardt annual reports to the USAF during their 1964 program.²⁰ A cluster of 24 regeneratively-cooled LOX/RP rockets forms the primary system, each with 2,960 lbf of thrust at standard conditions. Hydrocarbon injectors are used for the afterburner, which is downstream of the mixing chamber. Each engine weighs 5,300 lbm and generates 80,000 lbf of sea level static thrust (where augmentation is least effective). Ground-test data are available for a number of different equivalence ratios, secondary-to-primary flow ratios, mixer inlet Mach numbers, and flight Mach numbers, each for various propellant combinations. The engine data used in the present study were for primary chamber pressure of 600 psia, the primary and afterburner combustion chambers at stoichiometric equivalence ratio, and primary and afterburner chambers operating at 0.95 efficiency. Ground-test data showed that the secondary-to-primary flow ratio was the most significant influence on net thrust and specific fuel consumption, even more so than equivalence ratio or other factors; this verifies the advantage of using combined cycles.

While a more advanced full-scale version, the MA140-XAB, was also developed, the Marquardt MA139-XAA engine is the one that was chosen for use in the RBCC air-carrier trajectory simulations presented in the sections below. The decision was made to maintain hydrocarbon as the fuel for both the primary and afterburner combustion; a similar analysis could be performed for the LOX/LH2 primary and afterburner configurations.

B. The Pratt & Whitney J-58 Engine Representation

The J-58 engine for the SR-71 was a innovative marvel for its time (1950-1960s), using the most extreme materials available during that time period. After 50 years of technological development in materials research, however, the failure temperature and failure strength of a common commercial or military jet engine can now meet a large portion of the performance operation envelope (thrust, weight, fuel consumption) of the J-58 engine.¹⁴ Much of the mechanical hardware can now be replaced with much lighter electronic components, or done away with entirely.

The J-58 is a single-spool turbojet engine with an afterburner. Several modifications to the engine were made, however, in order to accommodate the performance envelope⁶ of the SR-71. The compressor was fitted with bypass tubing which was behind the fourth stage on the nine-stage compressor. The compressor face also had inlet guide vanes. These modifications were performed to prevent compressor stall at high speeds. By comparison, a modern turbojet engine now has several stages of variable compressor blades which can for the most part accomplish a similar purpose. The J-58 bypass tube fed directly into the afterburner, which actually caused flow reversal during engine start-up; this phenomenon was eventually offset by installing additional louvers (suck-in doors) on the main engine nacelle. The inlet was a highly-specialized movable spike which modulated according to the speed of the aircraft, along with other technological devices such as shock traps, forward and aft bypass doors and center-body bleeds. In addition, the rear of the engine was outfitted with a variable ejector nozzle with associated free-floating tertiary doors.

Many pieces of the J-58 technology can now be easily supplanted with the results of the past 40 to 50 years of engine technological evolution, such as digital engine controllers to replace hydromechanical control systems. These advancements would confer performance gains not modeled herein. In comparison to a modern engine, the Pratt & Whitney F100-PW-229 develops 29,160 lbf of afterburning thrust at standard temperature and pressure (STP), and has a dry weight of 3,740 lb with a thrust-to-weight ratio of 7.8:1; whereas the J58/JT11D-20A develops 32,000 lbf of afterburning thrust at STP, and has a dry weight of 6,000 lb, resulting in a thrust-to-weight ratio of 5.3:1. These numbers represent the core attributes of both engines and do not include the weight of variable-inlet machinery for either engine or the ejector nozzle on the J-58.²²

Can the historic configuration of the Pratt & Whitney J-58 with the Lockheed variable-geometry inlet be considered a true TBCC? From an aerospace purist view, the engine is never completely in a pure ramjet mode due to the fact that the first stages of compression are present before the mass flow is bypassed to the afterburner. In the viewpoint of the aerothermodynamist, however, the engine transitions through at least two modes or cycles and, thus, coupled with the turbine, can be classified as a TBCC.

III. Mission Trajectories and Performance

Trajectory optimization was performed using the RBCC and TBCC propulsion system models as installed onto a hypothetical supersonic carrier vehicle that was assumed to have the base aerodynamic model and propulsion performance of the SR-71 aircraft.²³ Test flights of the SR-71 carrying the LASRE indicate that such a carrier aircraft, encumbered with the additional drag of an external companion vehicle, would be able to achieve an approximate cruise condition of Mach 3.0 at an altitude of 70,000 ft.²⁴

The basis of any useful comparison between low-Earth orbit (LEO) access-to-space launch systems should be against a history of data on successful systems. The SpaceX (Space Exploration Technologies, Hawthorne, California) Falcon-1, a 61.5-klbf gross takeoff weight, LOX/RP system has successfully delivered a 165-kg (363-lb) payload into a 643- by 621-km (400- by 386-mi) LEO at an orbital inclination of 9.35 deg, and was chosen as the analysis reference point.

A POST model was constructed of the SpaceX Falcon-1 launch vehicle using information from the SpaceX payload User's Guide.²⁵ Several iterations were performed to attempt to match the first-stage performance using a ballistic model. Once the booster stage was successfully matched, the POST II optimizer was activated and the second stage was added to complete the simulation and deliver approximately 548 lbm into orbital conditions of an inertial velocity of 25,724 ft/s at an altitude of 520,997 ft and an inclination of 28.9 deg (corresponding to a launch from the NASA Kennedy Space Center, Florida).

For the airbreathing trajectories, constant dynamic pressure profiles as prescribed by Olds et al.²⁶ were implemented into POST and utilized. The minimum-fuel climb profiles²⁷ were also examined; the minimum-energy path and the adapted climb-dive procedure were examined to find the efficiency advantages in these cases. The Redin SR-71 climb-dive procedure²⁸ optimizes the ascent profile in the subsonic and transonic ascent region allowing for the added efficiency of lift, weight, thrust, and burn for the penetration of the sonic barrier. Once the sonic barrier is penetrated, the constant dynamic pressure profile is used to maximize the efficiency of supersonic airbreathing access-to-space ascent profiles until first-stage separation.

Trajectory modeling was performed according to the following criteria:

- The first-stage airbreathing trajectories were performed separately from the rocket ascent-to-orbit stages
- All first-stage airbreathing trajectory modeling in OTIS was performed with the OTIS 4.0.12 (build 545), SNOPT Version 7.2-5 optimizer ON
- All first-stage airbreathing trajectory modeling in POST II was performed with POST II Version 1.1.6.G, dated 12/15/04 with the optimizer OFF
- All rocket ascent-to-orbit trajectory modeling was performed in POST II Version 1.1.6.G, projected gradient method, with the optimizer ON.

A. Air Carrier Trajectories to Launch Condition

Trajectories for a hypothetical supersonic air-carrier vehicle were simulated to a practical launch point within known capability. The final mated booster aerodynamic model was assumed to be the SR-71 + LASRE configuration.

1. Turbine-Based Combined Cycle to SR-71 Cruise Condition

Initial modeling of the minimum fuel consumption climb profile²⁷ was performed using OTIS. This modeling did not include throttling, and the specific impulse was fixed at 1600 s. The OTIS modeling demonstrates, however, that there is some difference in the minimum fuel climb profile required for the baseline SR-71 and the SR-71 LASRE configuration. The constant dynamic pressure limit was increased from 700^{lbf}/ft² to 750^{lbf}/ft² for the OTIS SR-71 + LASRE model. The converged solution demonstrates that the pre-transonic penetration altitude differs from the baseline altitude by 33,000 ft to 41,000 ft.

In order to obtain more detailed verification, the climb profile was accomplished with the POST II modeling. In this case, a piece-wise approach using generalized acceleration steering was found to be the most stable method. The POST II SR-71 baseline strategy was to start at 400 KEAS at an altitude of 2000 ft, then hold the derivative of dynamic pressure constant at zero using alpha control as a single independent variable. For the constant-Mach climb beyond an altitude of 25,000 ft, the rate-of-change of Mach number

was used as a single dependent variable. The transonic dive was modeled with a constant flight path angle that terminated at 450 KEAS, and from then on the time rate of change of the dynamic pressure was once again used as a constant dynamic pressure climb to higher altitudes. The POST II SR-71 + LASRE piecewise trajectory was modeled as a constant Mach 0.9 subsonic climb, then a dive at an altitude of approximately 40,000 ft, followed by a constant dynamic pressure climb of $750 \text{ lb}_f/\text{ft}^2$ (470 KEAS) to the higher altitudes.

As indicated by the OTIS-optimized simulations, the initial height of the transonic penetration dive is higher for the LASRE configuration. There were also differences noted in the subsonic climb characteristics. The POST II level flight option in the generalized acceleration guidance module was used to determine the change in throttling characteristics. The baseline reached Mach 0.84 at an altitude 17,000 ft and then began a constant-Mach climb to 32,000 ft before performing a transonic penetration dive. A supersonic, constant dynamic pressure climb was initiated at Mach 1.2 and an altitude of 29,500 ft. It was found that the SR-71 LASRE climb model in POST II was very sensitive to small changes in altitude and Mach number.

The results of modeling the SR-71 indicate that Mach 3.0 at an altitude of 70,000 ft is a feasible separation condition and conforms with previous efforts, such as the MD-21/D-21 and LASRE experiments. Table 2 presents the difference in time and fuel consumption for the two climbs. In Table 2, all initial weights are 140,000 lbm and the final altitude was 70,000 ft. Final velocity was not held as a hard constraint. The trajectories of these ascent profiles in both OTIS and POST II, with and without the LASRE drag increment, are shown in Figure 6.

SR-71 configurations	Final weight, lbm	Total time, s	Final Mach number
OTIS baseline	119,120	1169	3.2
OTIS LASRE	113,348	1485	3.2
POST baseline	114,300	1631	3.0
POST LASRE	106,260	1627	3.0

Table 2. Results of OTIS and POST climb profiles indicating fuel consumption between the SR-71 baseline and the SR-71 LASRE configurations.

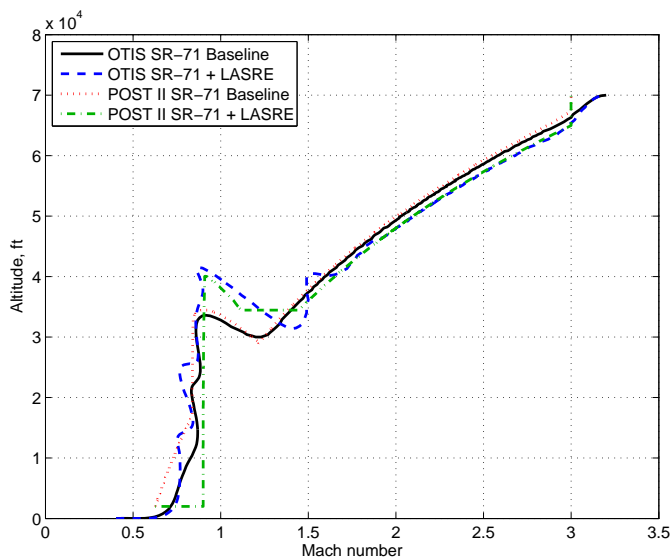


Figure 6. The OTIS (optimized) and POST II (piecewise non-optimized) minimum-energy climb profiles for the SR-71 and SR-71 + LASRE.

The fuel consumption during the transonic penetration is of interest; if the dive is accomplished with nominal fuel consumption the SR-71 could potentially have a range of payloads from 5000 lbm up to 30,000 lbm. A very optimistic number of 30,000 lbm payload depends on the mated drag characteristics. A more reasonable upper-end estimate for the SR-71 would be 15,000 lb. The purpose of this analysis, however, is to explore air-breathing booster access-to-space systems; thus it is reasonable to imagine a first-stage

airbreathing booster with a reduced drag configuration that can deliver 30,000 lbm to Mach 3.0 at an altitude of 70,000 ft. Therefore, for the second-stage-and-beyond, all-rocket system analysis the authors set the upper limit at 30,000 lbm. This limit also provides a future study design concept that includes the weight reduction of the airbreathing first stage. The SR-71 was mission-specific, thus, the boost stage was focused on second-stage access-to-space delivery and not necessarily on loitering or long-range reconnaissance, which would result in a different heat profile.

The payload-to-orbit stage will eventually require some form of apogee kick or upper-stage guidance; for simplicity a two-stage solid rocket was first considered. The generic method presented in Appendix C of Space Propulsion Analysis and Design²⁹ (SPAD) was first used to estimate the staging size, followed by the utilization of a trajectory construction method³⁰ to represent the actual systems that were possible. The POST II software was used as the trajectory analysis tool, with the final weight to orbit optimized by using inertial pitch as a control variable. Future studies could include optimization of burn sequencing; for now, the burn sequence and coast phase was manually performed by estimating the apogee and kick-fire timing. A generic 100-nm circular orbit was chosen as a reference. The results indicate that an airbreathing booster with a total dry system weight under 60,000 lb may very well demonstrate the economic effectiveness of an airbreathing first stage.

2. Rocket-Based Combined Cycle to SR-71 Cruise Condition

Using the model of the Marquardt MA139-XAA ejector ramjet engine, POST II simulations were performed of basic ascent trajectories to the estimated SR-71 + LASRE cruise condition of Mach 3.0 and an altitude of 70,000 ft. Each of the two J-58 engines from the TBCC model were replaced with an MA139-XAA engine, which started the flight profile in ejector ramjet mode (air-augmented rockets plus afterburning). A level acceleration from an initial condition of Mach 0.6 at an altitude of 2,000 ft was followed until a dynamic pressure of 450 KEAS (685 psf) was reached. The ascent then followed a constant dynamic pressure climb until attaining Mach 2.5, which is a feasible ramjet start velocity. At this point, mode-switching was performed to switch to pure ramjets (primary rockets off). Angle-of-attack guidance was then used to target specific final conditions of interest. The simulated ascent to the SR-71 cruise condition is shown in Figure 7(a).

The fuel-consumption advantage of using airbreathing propulsion is shown in Figure 7(b), in which the mode-switching point of approximately 76 s is immediately apparent in both thrust and specific impulse. While the available thrust is dramatically reduced when switching to the pure ramjet mode, the associated decrease in fuel consumption is similarly dramatic. Note that in a real ascent scenario, the ejector mode pure ramjet mode would most likely be transitioned much more smoothly using throttle control, which is not incorporated into these simulations. All simulations of the MA139-XAA in this paper are at constant, full throttle for both modes.

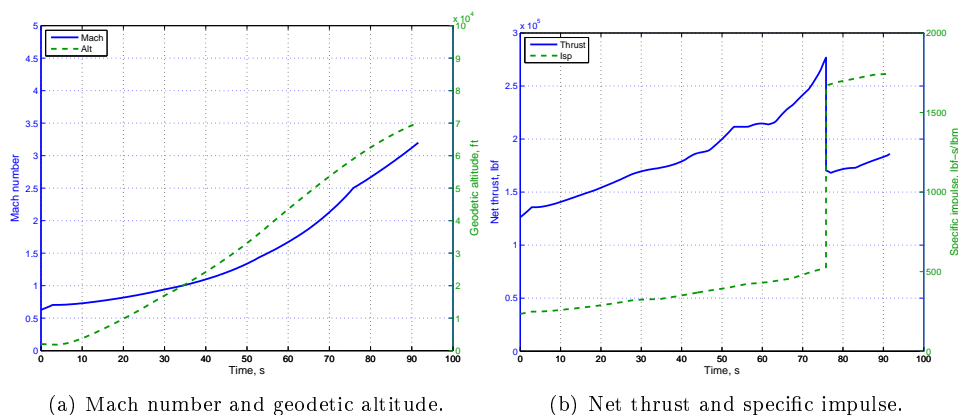


Figure 7. The simulated SR-71 ascent profile to Mach 3.2 and an altitude of 70,000 ft using the Marquardt MA139-XAA engine, with a staging point from ejector ramjet mode to pure ramjet mode at Mach 2.5 (approximately 76 s).

3. Rocket-Based Combined Cycle to Extended Launch Condition

It may generally be observed that a fair comparison between TBCC and RBCC systems would not necessarily involve the same staging point for the orbital insertion vehicle. If the trajectory is initially designed for the TBCC system, then an RBCC propulsion system flying to the same flight condition would be deprived of the regime for which it is best suited. The TBCC system will be more efficient than the ejector ramjet mode of an RBCC for the subsonic and low-supersonic portion of the ascent; however, the RBCC pure-ramjet mode can continue a very efficient, airbreathing ascent well into the Mach 4 to Mach 5 range, at altitudes exceeding 90,000 ft. Additionally, the increased mechanical complexity of the TBCC system is eliminated in the RBCC, providing a further advantage. Another possibility is a combined system that uses both engine systems: a TBCC system for ascent to a mid-supersonic staging point, followed by an RBCC pure ramjet mode climb to thin air, and finally the RBCC ejector mode and pure-rocket mode space entry.

An ascent profile for an example extended launch condition using the MA139-XAA engines is shown in Figure 8. This extended launch condition does not exceed the known dynamic pressure limit of 500 KEAS (approximately 850 psf) of the SR-71.

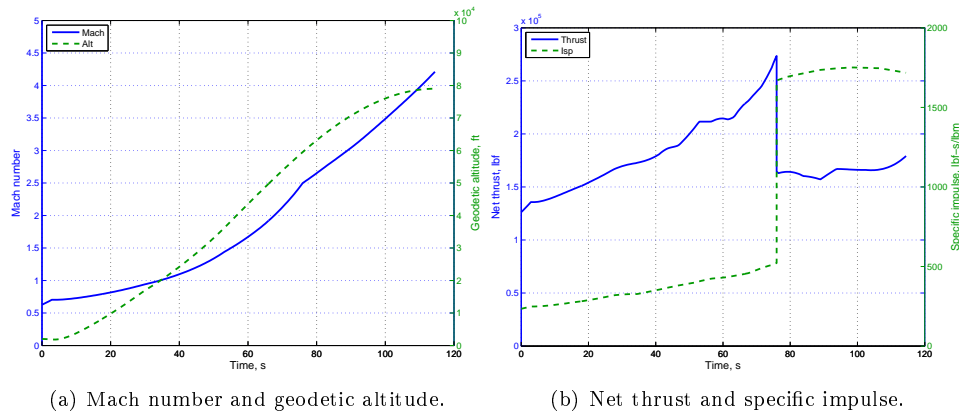


Figure 8. The simulated extended altitude and Mach number ascent profile to take advantage of the efficient, pure-ramjet-mode operation of the rocket-based combined-cycle engine.

B. Orbital Insertion Vehicle Trajectories from Launch Condition

Once the SR-71 based carrier vehicle has reached the chosen air-launch point, a rocket-based orbital insertion vehicle may be separated and launched. The carrier vehicle may then return to Earth and be refueled and re-equipped for another launch.

1. Baseline LOX/RP Rocket

The Falcon-1 system was modeled after the RatSat launch that occurred on September 28, 2008. The second stage uses LOX/RP and is solely a pressure-fed system with no turbo-pump. The system was modeled in POST II and several factors were adjusted to obtain a performance that was similar to the performance stated in the Space-X Falcon-1 User's Guide.²⁵

The thrust was adjusted to receive the correct weight of propellant expelled and burn time. There are various numbers that suggest that the gross weight differs from 60,440 to 61,500 lbm depending on the payload configuration; therefore, a mid-value of 61,000 lbm was selected. The original RatSat (364 lb) and RazakSat (397 lb) were early successful Falcon payloads which used two burn ascents instead of a direct insertion ascent. In this simulation, the direct burn is used and the orbit is circularized at 341.2 nm and 24750.7 ft/s. The second-stage thrust was adjusted for a burn time of 418 s. Various sources claim differing I_{sp} values and thrusts; for the simulation, approximately average values were used wherever possible. The final delivered payload weight for the normalized circular direct burn was 312 lb to orbit. These numbers fit closely with the representative curves given in the Space-X Falcon-1 User's Guide (figure 2-3 on page 15).²⁵ The vacuum thrust and specific impulse of the POST II Falcon-1 simulation are shown in Table 3.

	Thrust, lbf	I_{sp} , lbf -s/ lbm	Burn time, s
First stage	84100	300	169
Second stage	6600	314	418

Table 3. Normalized Falcon-1 POST II simulation parameters for a 341-nm circular orbit at 9.1 deg inclination, gross liftoff weight 61,000 lbm, and delivered payload 312 lbm.

The Falcon-1 calibrated, the insertion parameters were changed to a standard 100- by 100-nm orbit at 28.5 deg inclination. The Falcon system POST II simulation delivered approximately 763 lb to the standardized reference orbit; this is also consistent with performance predictions in the Space-X Falcon-1 User’s Guide. The trajectories for the Falcon-1 simulation in POST II are shown in Figure 9.

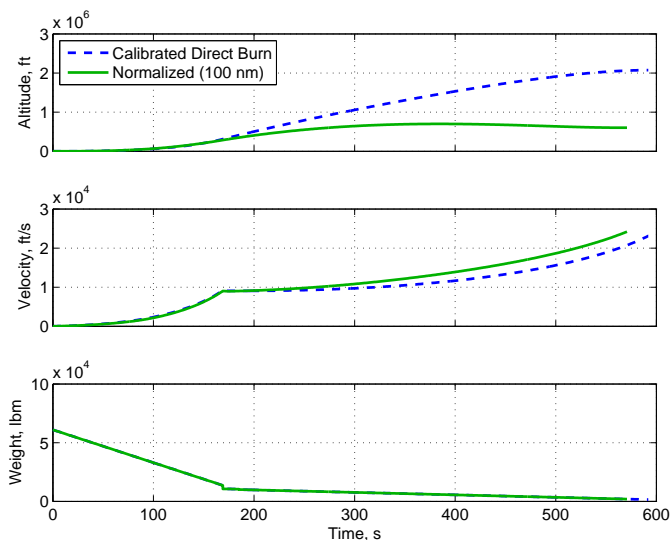


Figure 9. The geodetic altitude, velocity magnitude, and total launch vehicle weight compared with time for the simulated Falcon-1 ascent, shown for a calibrated direct burn and a normalized 100-nm circular orbit.

2. Upper-Stage Solid Rocket from Air Carrier

Solid rockets were examined because they are operationally simpler for both in-flight and ground considerations. Using the ratio of delta velocities method defined in SPAD (page 722), the weights, burn times, and thrusts were determined for generic classes of a two-stage solid rocket system launched from Mach 3.0 at an altitude of 70,000 feet. Several parameters were fixed based on two known available solid rockets, the Orion50XL and the Star20. The first- and second-stage specific impulses were taken from the Orion50XL (289 s) and the Star20 (284 s). Although newer solid rockets have appeared on the market, such as the Oriole ($I_{sp} = 306$ s), the lower, more conservative values for specific impulse were used because they were thought to be more practical. Thrust and burn time were determined by estimating the first-stage acceleration at 3.33 G’s using gross system weight and the second stage at 4 G’s using the second-stage gross weight. A spreadsheet solver function was used to optimize the ratio of delta velocities. Burn times for the two stages were both approximately 64 to 65 s. The inert mass fractions of the first and second stages were 0.0876 and 0.09172, respectively.

Table 4 shows the results of the generic solid rocket study, with the normalized orbit being 100 nm circular at 28.5 deg inclination. The flight path angle was set conservatively at $\gamma = 0$, although previous studies¹⁷ suggest that the flight path angle can be slightly more at $\gamma = 1.2$.

Two commercial solid rocket systems were composed to match the performance shown in the generic table. In general, it was concluded that a second stage would require propellant offloading in order to match those parameters. The results can be seen in Table 5. Since it is not easy to change the manufacturing parameters of the solid rocket casing and nozzles, optimal conditions are not necessarily achieved.

Weight class, lbm	First-stage weight, lbm	First-stage thrust, lbf	Second-stage weight, lbm	Second-stage thrust, lbf	Payload to orbit, lbm
5000	4117	16650	711	2843	210
10000	8233	33300	1421	5686	432
15000	12350	49950	2132	8528	657
20000	16467	66500	2843	11371	882
25000	20583	83250	3553	14214	1095
30000	24700	99900	4264	17057	1330

Table 4. Payload delivered to a 100-nm circular orbit by a generic two-stage solid rocket system from a launch point of Mach 3.0 at an altitude of 70,000 ft.

Weight class, lbm	First-stage weight, lbm	First-stage, thrust, lbf	Second-stage weight, lbm	Second-stage thrust, lbf	Payload to orbit, lbm
Orion50XL+Star20					
10214	9551	34500	663	6100	355
Orion50XL+3XStar20s					
11540	9551	34500	1989	6100	524

Table 5. Payload delivered to a 100-nm circular orbit by a commercially-composed two-stage solid rocket system from a launch point of Mach 3.0 at an altitude 70,000 ft.

3. Upper-Stage LOX/RP Rocket from Air Carrier

The Falcon-1 was also used as a baseline for the upper, liquid-fueled stages (launching from ground to orbit) because it was close to the weight class range needed for the second stage of the composed air launch system.²⁵ A review of the existing market of liquid-fueled rockets in the size range indicates that it would be difficult to find a suitable weight system that also reaches the reference orbital velocity. Therefore, the method presented in SPAD was also applied to generic case of liquid-fueled rockets. In this case the inert mass fraction ratios of the Falcon-1 were used to generate the generic performance tables. The generic liquid-fueled POST II analysis (Table 6 below) allows the reader to understand the performance capabilities associated with liquid systems. For reference, payload performance of the ground-to-orbit Falcon-1 61-klbf gross liftoff weight (GLOW) system falls between the 10-klbf and 15-klbf air-carrier-launched systems in Table 6.

Weight class, lbm	First-stage weight, lbm	First-stage thrust, lbf	Second-stage weight, lbm	Second-stage thrust, lbf	Payload to orbit, lbm
5000	4116	16650	710	2843	243
10000	8350	33300	1196	4786	563
15000	12525	49950	1795	7179	844
20000	16700	66700	2293	9572	1133
25000	20875	83250	2991	11965	1421
30000	25050	99900	3589	14358	1711

Table 6. Payload delivered to a 100-nm circular orbit by a generic two-stage liquid-fueled rocket system from a launch point of Mach 3.0 at an altitude of 70,000 ft.

An additional analysis was performed to consider the payload to orbit launched from an air carrier at the extended RBCC flight condition described in Section 3.A. The results of this analysis are shown in Table 7.

Weight class, lbm	First-stage weight, lbm	First-stage thrust, lbf	Second-stage weight, lbm	Second-stage thrust, lbf	Payload to orbit, lbm
10000	8350	33300	1196	4786	619
20000	16700	66700	2293	9572	1329
30000	25050	99900	3589	14358	2006

Table 7. Payload delivered to a 100-nm circular orbit by a generic two-stage liquid-fueled rocket system from the simulated rocket-based combined-cycle (RBCC) extended launch point of Mach 4.25 at an altitude of 80,000 ft, selected to take advantage of the extended Mach number capability of the RBCC.

IV. Research and Development Pathway

The key to advancing RBCC and TBCC technology to the level acceptable for access-to-space applications is the acquisition of high-quality, relevant, and, to the greatest degree possible, comprehensive flight data. Model fidelity may be improved by way of various theoretical means, but flight is the only aeronautical reality. Parametric cycle analysis, computational fluid dynamics, and other forms of modeling must be validated by comparison to flight, such that they may be used with confidence in the design and development of tomorrow's airbreathing access-to-space systems. The value of flight goes beyond merely validating an existing model; it is limiting to consider validation as the only purpose of flight research. Indeed, the term "flight research" (as opposed to "flight test") implies an active process of exploration: technical hurdles are measured and analyzed, creative solutions are hypothesized and tested, and the process is adjusted and then repeated in the quest for understanding of new phenomena.

A. Past and Present Flight Research Efforts

Combined cycle and related propulsion work at NASA DFRRC has been centered on the Propulsion Flight Test Fixture,³¹ which is an instrumented pylon designed for cold- and hot-fire, in-flight-testing of propulsion systems and components underneath a NASA F-15B testbed aircraft. Experiments began with the Local Mach Investigation³² project, which sought to ascertain local flow Mach number underneath the F-15B. In 2008, the Rake Airflow Gage Experiment (RAGE) was designed and calibrated³³ to probe local Mach number and flow angularity at the aerodynamic interface plane, located at the cowl face, of a novel mixed-compression supersonic inlet. The RAGE was flown in 2009³⁴ and is shown in Figure 10.

Using data from the RAGE flights, the Channeled Centerbody Inlet Experiment (CCIE)³⁵ was designed and is planned to be flown in calendar year 2011. The CCIE will explore the off-design performance and inlet face distortion of this variable-geometry, mixed-compression inlet technology. The CCIE was designed to provide proper mass flow and starting for the previously-mentioned RBCC engine DRACO.¹ The DRACO engine in its original form does not exist today as a program, but similar efforts would be straightforward to revive and could be natural follow-on subjects of experimentation to the present CCIE research.

The NASA DFRRC also began a research program called the Ducted Rocket EXperiment, or D-REX. The D-REX project sought to explore flow dynamics related to ramjet ejector mode operation.

B. The Pathway to Flight-Testing Combined-Cycle Engines

Combined-cycle engines, are, by their nature, cross-cutting and integrated technologies. Because airbreathing access-to-space is among their applications, entities that are developing new space exploration systems would have an interest in the end products of combined-cycle engine advancement. Gas turbine and ram-and scramjet engine development have been traditionally the domain of the aeronautics side of the of the aerospace research community, and much of the needed research work lies within the domain of the aeronautics establishment. Combined-cycle engine research is cross-cutting within aeronautics as well; TBCC engines cover the subsonic and supersonic regimes, and RBCC engines can enter hypersonic and rarefied flow regimes as well.

Barber, Maicke, and Majdalani³⁶ identified Gaps, Obstacles, and Technological Challenges in Hypersonic Applications (GOTCHA) which are impeding technological progress in combined-cycle and other high-speed propulsion systems. Among the list of aerodynamic, propulsive, testing, modeling, and materials problems are many areas of technological advancement that require component-level or integrated system flight re-



Figure 10. A NASA Dryden Flight Research Center F-15B shown in flight with the Rake Airflow Gage Experiment attached to the Propulsion Flight Test Fixture.

search to reach a readiness level appropriate for an operational vehicle powered by combined-cycle engines. In particular, while they note that full integrated flight-testing is typically an expensive (but valuable) proposition, they go on to identify smaller test articles for flight validation and faster turnaround times as capabilities that would greatly enhance the progress of high-speed propulsion systems. Platform-based modular test systems such as the Propulsion Flight Test Fixture at NASA DFRC could help address this gap.

According to the roadmaps published by the Joint Technology Office (JTO) on Hypersonics,³⁷ modeling of high-speed combustion dynamics and boundary layer transition in the Mach range specified is of particular interest. Three further objectives in the JTO roadmaps are the “ability to rapidly and accurately simulate variable-Mach airflow using variable geometric structures to constrict or expand the airflow in response to testing requirements,” the “ability to rapidly and accurately simulate airflow transients to assess impact on aerodynamics and propulsion using variable geometric structures,” and the “ability to obtain in-stream measurements to assess combustion processes on a vehicle under test.”³⁷ The final JTO goals in the “Basic Research” section of the roadmap document contain three additional areas of research that would be required for RBCC and other hypersonic systems development: supersonic combustion, boundary layer physics, and shock-dominated flows.

The use of computational fluid dynamics simulation and other numerical modeling techniques to analyze these phenomena will require validation with real flight data to provide meaningful input to more involved design efforts for future launch vehicles, which are of great interest to the research community and the United States Government. Validation of certain aspects of these goals do not explicitly require high-supersonic or hypersonic flight, but could be tested at low-supersonic speeds and applied to moderately higher ones. Flight-testing an RBCC-type engine or its subcomponents, or both, at subsonic and low-supersonic Mach numbers would go a long way toward providing validation data for ongoing modeling efforts and future potential flight research programs.

After the component level technologies are validated through flight, additional flight research can begin the study of less-explored flight regimes. Such regimes include the Mach 2 to Mach 5 “gap,” in which neither the supersonic civil transport community (Mach 1 to Mach 2) nor the hypersonic scramjet community (Mach 5 to Mach 10 and above) have shown much interest. Yet it is in this gap that much of the required technology development, such as engine mode switching, resides.

Olds⁹ in 1999 outlined two proposed methods of bringing RBCC engines to flight-testing. The first method was to use the X-34 suborbital, unmanned rocketplane³⁸ as a testbed vehicle for an ejector scramjet.

Today, just over a decade later, the X-34 vehicles were recently towed from storage at Edwards Air Force Base (Edwards, California) for evaluation as potential suborbital research and test vehicles. If the X-34 vehicles themselves cannot be used, they can serve as useful examples of existing systems that could be adapted for the purpose of bringing specific combined-cycle engine technologies to flight research.

C. Concluding Remarks

No matter the specific steps, the general principle should hold that the fastest and most effective pathway to flight research for a particular technology is to refrain from incorporating as many unknown and unproven systems as possible. The leap to fully-integrated, completely new systems may appear to yield more advancement at a faster rate; however, systems such as these have been shown to approach prohibitive technical and budgetary complexity very rapidly. Simpler systems with more modest goals of advancing specific technologies, such as combined-cycle engines, would perhaps lead to more practical flight research objectives while still retaining the capability to advance innovations in the field in a spiral of technological development.

This paper has described the development of engine models and ascent trajectories that demonstrate that existing systems (in fact, systems that have existed for as long as five decades) are at least nominally capable of providing airbreathing space access for practical payload sizes. Turbine-based combined-cycle (TBCC) engines are flight-proven in legacy and modern systems, and rocket-based combined-cycle (RBCC) engines have been fully ground-tested and merely await flight research to bring them to the next level of technology readiness. Innovations garnered from flight research of both TBCC and RBCC engines will enable further advancement in game-changing, airbreathing, and horizontal-launch space-access concepts.

References

- ¹Hueter, U., "Rocket-Based Combined-Cycle Propulsion Technology for Access-to-Space Applications," AIAA 1999-4925, 1999.
- ²Liu, Z., Wang, Z., and Cai, Y., "Integrated Performance Numerical Simulation of Hypersonic Vehicle and Turbine Based Combined Cycle Propulsion System," AIAA 2009-5299, 2009.
- ³Daines, R., "Combined Rocket and Airbreathing Propulsion Systems for Space-Launch Applications," *Journal of Propulsion and Power*, Vol. 14, No. 5, 1998, pp. 605-612.
- ⁴Chase, R. L. and Tang, M., "The Quest for a Robust, Responsive, Reliable, Efficient And Low Cost Space Access Capability," AIAA 2009-7417, 2009.
- ⁵Odegaard, E. and Stroup, K., "Advanced Ramjet Concepts," Air Force Aero Propulsion Laboratory, Technical Report, AFAPL-TR-67-118, Volume III, 1966.
- ⁶Merlin, P., *Form Archangel to Senior Crown: Design and Development of the Blackbird*, American Institute of Aeronautics and Astronautics, 2008.
- ⁷Brauer, G., Cornick, D., and Stevenson, R., "Capabilities and Applications of the Program to Optimize Simulated Trajectories (POST)," NASA CR-2770, 1977.
- ⁸Paris, S. and Hargraves, C., "Optimal Trajectories by Implicit Simulation OTIS, Volume II - User's Manual," available from NASA Glenn Research Center, Cleveland, Ohio 44135, 1986.
- ⁹Olds, J. R., "Two Options for Flight Testing Rocket-Based Combined-Cycle Engines," *Journal of Spacecraft and Rockets*, Vol. 36, No. 5, 1999.
- ¹⁰Mankins, J. C., Howell, J., and Olds, J. R., "Combined Airbreathing/Rocket Powered Highly Reusable Space Transport Flight Profiles: A Progress Report," AIAA 96-4516, 1996.
- ¹¹Olds, J. R., "Options for flight testing rocket-based combined-cycle (RBCC) engines," AIAA 96-2688, 1996.
- ¹²Perkins, H. D., Thomas, S. R., and Pack, W. D., "Mach 5 to 7 RBCC propulsion system testing at NASA-LeRC HFT," AIAA 97-0565, 1997.
- ¹³Trefny, C. J. and Roche, J. M., "Performance Validation Approach for the GTX Air-Breathing Launch Vehicle," NASA/TM-2002-211495, 2002.
- ¹⁴Mattingly, J., *Elements of Propulsion: Gas Turbines and Rockets*, AIAA Education Series, 2006.
- ¹⁵Tang, M. and Chase, R. L., "The Quest for Hypersonic Flight with Air-Breathing Propulsion," AIAA 2008-2546, 2008.
- ¹⁶Young, D. A. and Olds, J. R., "Responsive Access Small Cargo Affordable Launch (RASCAL) Independent Performance Evaluation," AIAA 2005-3241, 2005.
- ¹⁷Anderson, E. C. and Lopata, J. B., "Using a modified SR-71 aircraft and air-launched expedable rockets to place small payloads into orbit," AIAA 96-2774, 1996.

- ¹⁸Lockheed Aircraft Corporation, "Handling Qualities of the SR-71," Advanced Development Projects, Report SP-508, 1964.
- ¹⁹"SR-71A Flight Manual, Section 2, "Normal Procedures"," T.O. SR-71A-1, 1989.
- ²⁰Totten, J., "Final Summary Technical Report on the Calendar Year 1963 Ramjet Technology Program, Vol II," Marquardt Corporation, Report No. 25,116, 1964.
- ²¹Klann, J.L. and Snyder, C.A., "NEPP Programmers Manual (NASA Engine Performance Program), Volume 1. Technical Description," NASA Technical Memorandum 106575, 1994, available from the Aerospace Analysis Office, Lewis Research Center, Cleveland Ohio.
- ²²Pratt & Whitney Aircraft, "Installation Handbook JT11-J58 High-Mach-Number Turbojet Engine," July, 1959.
- ²³Meyer, J., McMaster, J., and Moody, R., "Handling Qualities of the SR-71 (Revised)," Lockheed Aircraft Corporation SP-508, 1978.
- ²⁴Corda, S., Moes, T. R., Mizukami, M., Hass, N. E., Jones, D., Monaghan, R. C., Ray, R. J., Jarvis, M. L., and Palumbo, N., "The SR-71 Test Bed Aircraft: A Facility for High-Speed Flight Research," NASA/TP-2000-209023, 2000.
- ²⁵Space Exploration Technologies, "Falcon 1 Launch Vehicle Payload User's Guide," Revision 7.
- ²⁶Olds, J. R., Bradford, J. E., Charania, A., Ledsinger, L., McCormick, D., and Sorenson, K., "Hyperion: An SSTO Vision Vehicle Concept Utilizing Rocket-Based Combined-Cycle Propulsion," AIAA 99-4944, 1999.
- ²⁷Rutowski, E. S., "Energy Approach to the General Aircraft Performance Problem," *Journal of the Aeronautical Sciences*, , No. 21, 1954, pp. 187-195.
- ²⁸Redin, P., "Optimization of Transonic Acceleration Performance for the YF-12C Airplane Using the Climb-Dive Maneuver," NASA TM-X-2694, 1979.
- ²⁹Humble, R. W., Henry, G. N., and Larson, W. J., *Space Propulsion Analysis and Design*, The McGraw-Hill Companies, Inc, 1995.
- ³⁰Kloesel, K. J., Pickrel, J. B., Sayles, E. L., Wright, M., Marriott, D., Holland, L., and Kuznetsov, S., "First Stage of a Highly Reliable Reusable Launch System," AIAA 2009-6805, 2009.
- ³¹Corda, S., Vachon, M., Palumbo, N., Diebler, C., Tseng, T., Ginn, A., and Richwine, D., "The F-15B Propulsion Flight Test Fixture : A New Flight Facility for Propulsion Research," AIAA 2001-3303, 2001.
- ³²Vachon, M. J., Moes, T. R., and Corda, S., "Local Flow Conditions for Propulsion Experiments on the NASA F-15B Propulsion Flight Test Fixture," NASA/TM-2005-213670, 2005.
- ³³Flynn, D. C., Ratnayake, N. A., and Frederick, M., "Design and Calibration of a Flowfield Survey Rake for Inlet Flight Research," AIAA-2009-1484, 2009.
- ³⁴Frederick, M. A. and Ratnayake, N. A., "Flight Test Results from the Rake Airflow Gage Experiment on the F-15B Airplane," AIAA-2010-4573, 2010.
- ³⁵Ratnayake, N. A., "Analysis of a Channeled Centerbody Supersonic Inlet for F-15B Flight Research," AIAA 2010-477, 2010.
- ³⁶Barber, T. A., Maicke, B. A., and Majdalani, J., "Current State of High Speed Propulsion: Gaps, Obstacles, and Technological Challenges in Hypersonic Applications," AIAA 2009-5118, 2009.
- ³⁷Outz, P., "The Joint Technology Office on Hypersonics," AIAA-2008-2576, 2008.
- ³⁸Sullivan, R. B. and Winters, B., "X-34 Program Overview," AIAA-1998-3516, 1998.



A Technology Pathway for Airbreathing, Combined-Cycle, Horizontal Space Launch Through SR-71 Based Trajectory Modeling

Kurt J. Kloesel, Nalin A. Ratnayake, and Casie M. Clark

NASA Dryden Flight Research Center, Edwards AFB,
California, 93523



Questions?

- Hugh L. Dryden – “...Separate the real from the imagined...”
- Modern day expression- “Flight is the only Truth!”
- Questions?

Air-Breathing Access to Space

The Holy Grail of Aeronautics

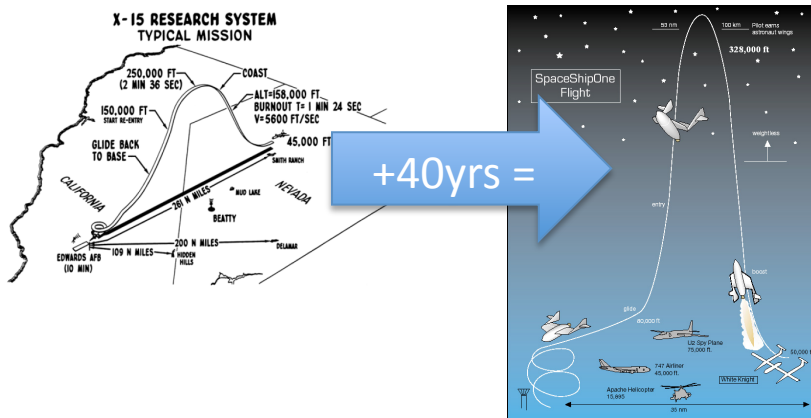


Graphics courtesy of NASA-Langley Hypersonics Office



Commercialization of Space

- Current movement towards commercialization
 - X-15 + 40 years = White Knight
 - Mercury-Atlas + 40 years = SpaceX FALCON
 - SR-71 + ? years = operational supersonic air-breathing access-to-space infrastructure



Observation: Use existing technology/vehicle systems already developed and flight proven.



Economic Reality of Air Breathing Space Access

Rand Corp. Study on Military Jet Acquisition

Table 6.12

Results of the Estimating Relationships for the Two Notional Engines

	New Engine (2001 Dollars)	Derivative Engine (2001 Dollars)
Development costs	\$4,840 million	\$780 million
Development time	51 months	33 months
Production cost for engine (T ₁)	\$14.3 million	\$8.67 million
Production cost for engine (T ₃₇₅)	\$5.8 million	\$5.6 million

Observation: New engine development is very expensive, the development of a new, high mach number air-breathing carrier would be enormously expensive. Consider using existing technology.

Source: "Military Jet Engine Acquisition Technology Basics and Cost-Estimating Methodology by Obaid Younossi, Mark V. Arena, Richard M. Moore Mark Lorell, Joanna Mason, John C. Graser", Rand Corp., United States Air Force under Contract F49642-01-C-0003, ISBN 0-8330-3282-8 (pbk.) year 2002".



Analysis Objectives

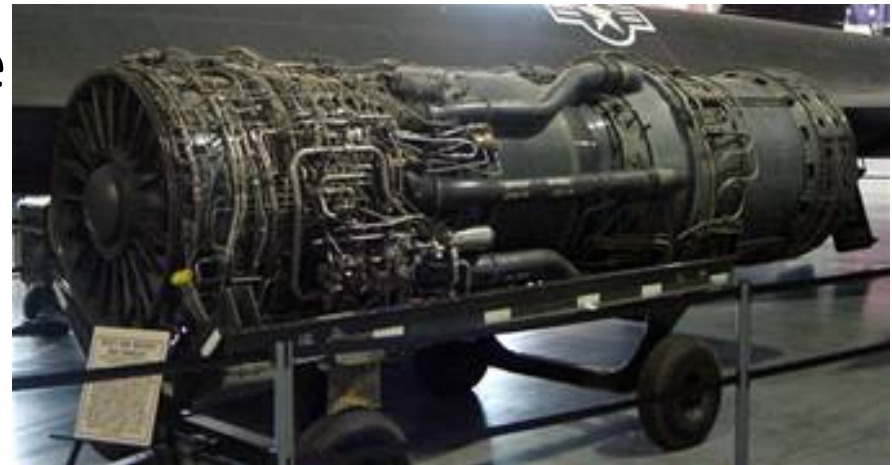
- Examines the technical performance aspects of the commercialization of an air-breathing booster stage
- Performance comparison between air breathing booster system and LOX-RP all rocket system



Turbojets: 50 years of improvements

J-58/JT11D-20A Performance

- 32,000 lbf of afterburning thrust at STP
- dry weight of 6,000 lb
- thrust-to-weight ratio of 5.3:1.



F100-PW-229 Performance

- 29,160 lbf of afterburning thrust at STP
- dry weight of 3,740 lb
- thrust-to-weight ratio of 7.8:1



These numbers represent the core attributes of both engines and do not include the weight of variable-inlet machinery for either engine or the ejector nozzle on the J-58

3/14/2011 K.J.Kloesel



Engines: Decades of Technological Improvements

Many pieces of the J-58 technology can now be easily supplanted with the results of the past 40 to 50 years of engine technological evolution, such as digital engine controllers to replace hydromechanical control systems.

The J-58 engine for the SR-71 was a innovative marvel for its time (1950-1960s), using the most extreme materials available during that time period. After 50 years of technological development in materials research, however, the failure temperature and failure strength of a common commercial or military jet engine can now meet a large portion of the performance operation envelope (thrust, weight, fuel consumption) of the J-58 engine. Much of the mechanical hardware can now be replaced with much lighter electronic components, or done away with entirely.

Table 6.2 Component efficiencies, total pressure ratios, and temperature limits

Component	Figure of merit	Type ^a	Level of technology ^b			
			1	2	3	4
Diffuser	π_{dmax}	A	0.90	0.95	0.98	0.995
		B	0.88	0.93	0.96	0.98
		C	0.85	0.90	0.94	0.96
Compressor	e_c		0.80	0.84	0.88	0.90
Fan	e_f		0.78	0.82	0.86	0.89
Burner	π_b		0.90	0.92	0.94	0.95
Turbine	η_b	Uncooled	0.88	0.94	0.99	0.999
		Cooled	0.80	0.85	0.89	0.90
Afterburner	π_{AB}		0.90	0.92	0.94	0.95
	η_{AB}		0.85	0.91	0.96	0.99
Nozzle	π_n	D	0.95	0.97	0.98	0.995
		E	0.93	0.96	0.97	0.98
		F	0.90	0.93	0.95	0.97
Mechanical shaft	η_m	Shaft only	0.95	0.97	0.99	0.995
		With power takeoff	0.90	0.92	0.95	0.97
Maximum T_{t4}		(K)	1110	1390	1780	2000
		(R)	2000	2500	3200	3600
Maximum T_{t7}		(K)	1390	1670	2000	2220
		(R)	2500	3000	3600	4000

^aA = subsonic aircraft with engines in nacelles D = fixed-area convergent nozzle
 B = subsonic aircraft with engine(s) in airframe E = variable-area convergent nozzle
 C = supersonic aircraft with engine(s) in airframe F = variable-area convergent-divergent nozzle
^bNotes: Stealth may reduce π_{dmax} , π_{AB} , and π_n . The levels of technology can be thought of as representing the technical capability for 20-yr increments in time beginning in 1945. Thus level 3 of technology presents typical component design values for the time period 1985–2005.

Observation: Consider using existing technology.

Source: Elements of Propulsion, Gas Turbines and Rockets, J.D. Mattingly, 2nd edition , 2006 AIAA Education Series, ISBN 1-56347-779-3



Mission Trajectories and Performance

Trajectory modeling was performed according to the following criteria:

- The first-stage airbreathing trajectories were performed separately from the rocket ascent-to-orbit stages
- All first-stage airbreathing trajectory modeling in OTIS was performed with the OTIS 4.0.12 (build 545), SNOPT Version 7.2-5 optimizer ON
- All first-stage airbreathing trajectory modeling in POST II was performed with POST II Version 1.1.6.G, dated 12/15/04 with the optimizer OFF
- All rocket ascent-to-orbit trajectory modeling was performed in POST II Version 1.1.6.G, projected gradient method, with the optimizer ON.



SR-71 + LASRE Model Performance Calibration

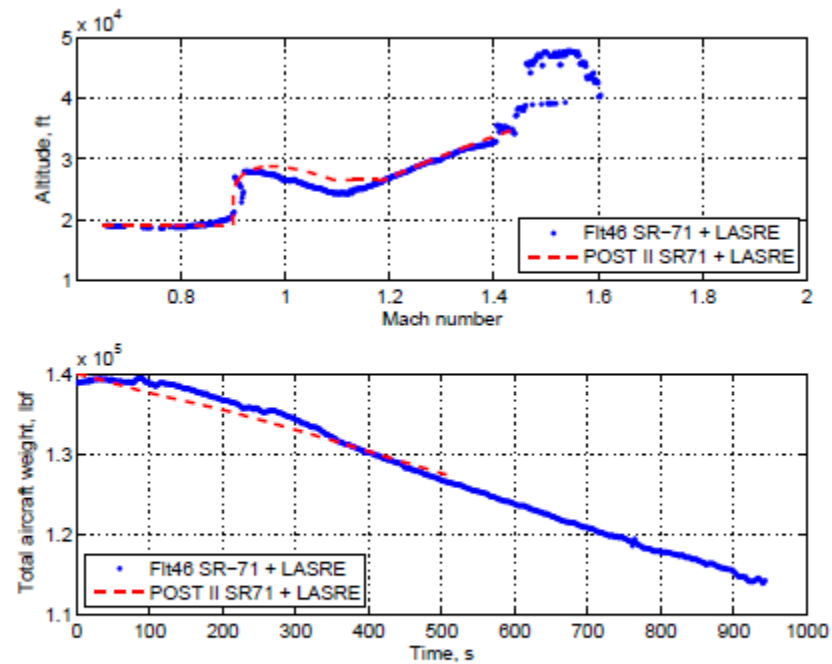


Figure 2. Aerodynamic model validation case in POST II compared to data from Flight 46 of the SR-71 with the LASRE.





SR-71 Performance Modeling

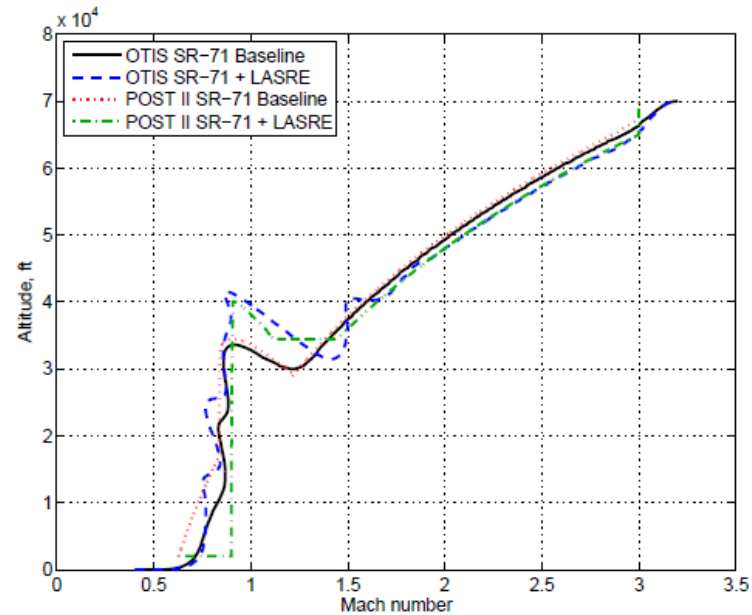


Figure 6. The OTIS (optimized) and POST II (piecewise non-optimized) minimum-energy climb profiles for the SR-71 and SR-71 + LASRE.

SR-71 configurations	Final weight, lbm	Total time, s	Final Mach number
OTIS baseline	119,120	1169	3.2
OTIS LASRE	113,348	1485	3.2
POST baseline	114,300	1631	3.0
POST LASRE	106,260	1627	3.0

Table 2. Results of OTIS and POST climb profiles indicating fuel consumption between the SR-71 baseline and the SR-71 LASRE configurations.



Baseline LOX/RP All Rocket to LEO Performance

The Falcon-1 system was modeled after the RatSat launch that occurred on September 28, 2008. The second stage uses LOX/RP and is solely a pressure-fed system with no turbo-pump. The system was modeled in POST II and several factors were adjusted to obtain a performance that was similar to the performance stated in the Space-X Falcon-1 User's Guide.

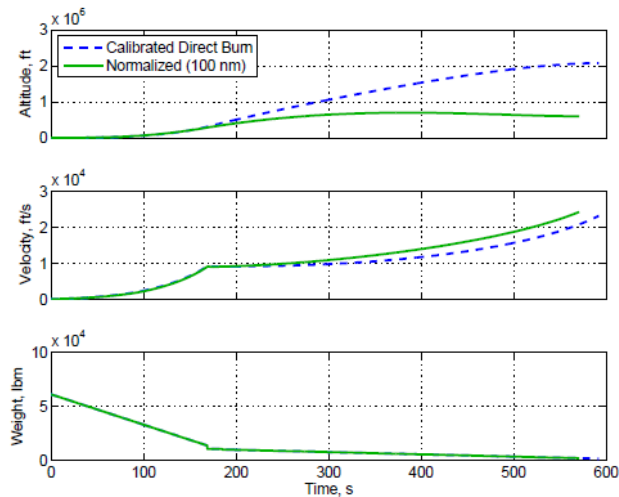


Figure 9. The geodetic altitude, velocity magnitude, and total launch vehicle weight compared with time for the simulated Falcon-1 ascent, shown for a calibrated direct burn and a normalized 100-nm circular orbit.

The Falcon-1 calibrated, the insertion parameters were changed to a standard 100- by 100-nm orbit at 28.5 deg inclination. The Falcon system POST II simulation delivered approximately 763 lb to the standardized reference orbit; this is also consistent with performance predictions in the Space-X Falcon-1 User's Guide.

The thrust was adjusted to receive the correct weight of propellant expelled and burn time. There are various numbers that suggest that the gross weight differs from 60,440 to 61,500 lbm depending on the payload configuration; therefore, a mid-value of 61,000 lbm was selected. The original RatSat (364 lb) and RazakSat (397 lb) were early successful Falcon payloads which used two burn ascents instead of a direct insertion ascent. In this simulation, the direct burn is used and the orbit is circularized at 341.2 nm and 24750.7 ft/s. The second-stage thrust was adjusted for a burn time of 418 s. Various sources claim differing I_{sp} values and thrusts; for the simulation, approximately average values were used wherever possible. The final delivered payload weight for the normalized circular direct burn was 312 lb to orbit. These numbers fit closely with the representative curves given in the Space-X Falcon-1 User's Guide (figure 2-3 on page 15).

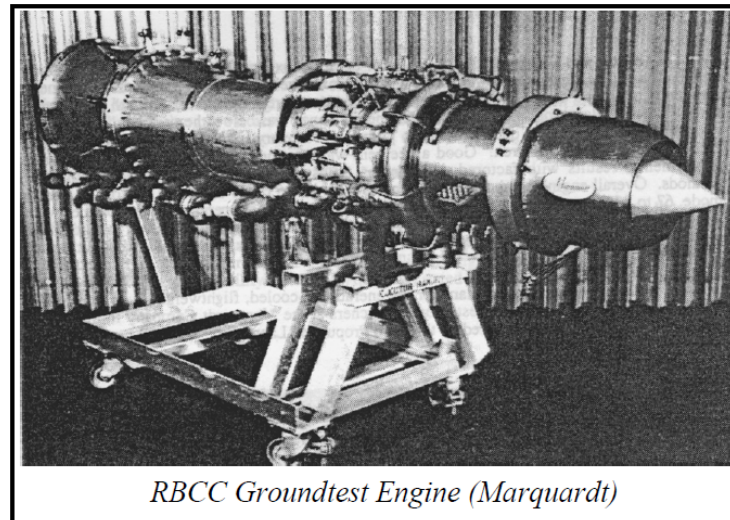


Marquardt MA139-XAA Ejector Ramjet

RBCC Performance

MA139-XAA engine, Ejector ramjet 80,000 lbf @ STP liquid oxygen & rocket propellant (LOX/RP) primary(rocket) combustors, hydrocarbon fuel afterburner.

A cluster of 24 regeneratively-cooled LOX/RP rockets forms the primary system, each with 2,960 lbf of thrust at standard conditions. Hydrocarbon injectors are used for the afterburner, which is downstream of the mixing chamber. Each engine weighs 5,300 lbf and generates 80,000 lbf of sea level static thrust (where augmentation is least effective). Ground-test data are available for a number of different equivalence ratios, secondary-to-primary flow ratios, mixer inlet Mach numbers, and flight Mach numbers, each for various propellant combinations. The engine data used in the present study were for primary chamber pressure of 600 psia, the primary and afterburner combustion chambers at stoichiometric equivalence ratio, and primary and afterburner chambers operating at 0.95 efficiency.



RBCC Groundtest Engine (Marquardt)



GE-CAT Ejector Ramjet Engine Modeling

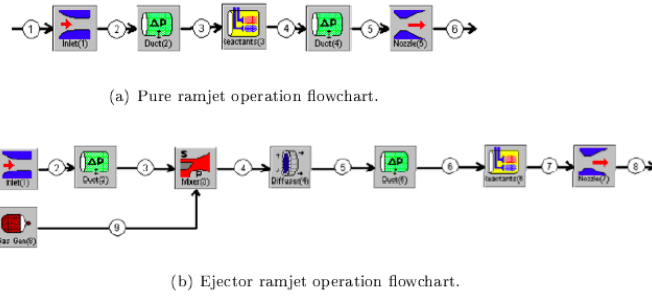


Figure 3. Flowchart of the Graphical Engine Cycle Analysis Tool model for the subscale Marquardt ejector ramjet.

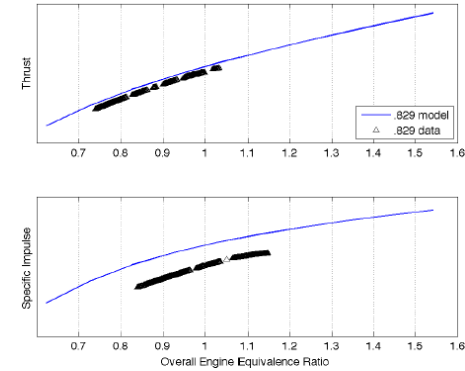


Figure 5. The Graphical Engine Cycle Analysis Tool rocket-based combined-cycle model estimates of sea level Mach 1.9 thrust and specific impulse compared with the overall engine equivalence ratio, plotted against Marquardt Corporation test data.

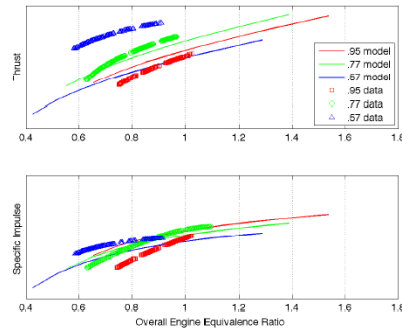


Figure 4. The Graphical Engine Cycle Analysis Tool rocket-based combined-cycle model estimates of sea level static thrust and specific impulse compared with the overall engine equivalence ratio, plotted against Marquardt Corporation test data.

Model error	Net thrust, percent	I_{sp} , percent
Static $\Phi_r = 0.95$	4.89	6.48
Static $\Phi_r = 0.77$	2.46	2.07
Static $\Phi_r = 0.57$	19.94	4.52
Mach 1.9 (ejector), $\Phi_r = 0.829$	2.09	6.58
Mach 1.9 (ramjet), $\Phi_r = 0.829$	5.25	8.47

Table 1. Average error versus Marquardt Corporation engine data for the Graphical Engine Cycle Analysis Tool rocket-based combined-cycle model at certain Mach numbers, configurations, and primary (rocket) equivalence ratios.



Rocket-Based Combined Cycle to SR-71 Cruise Condition

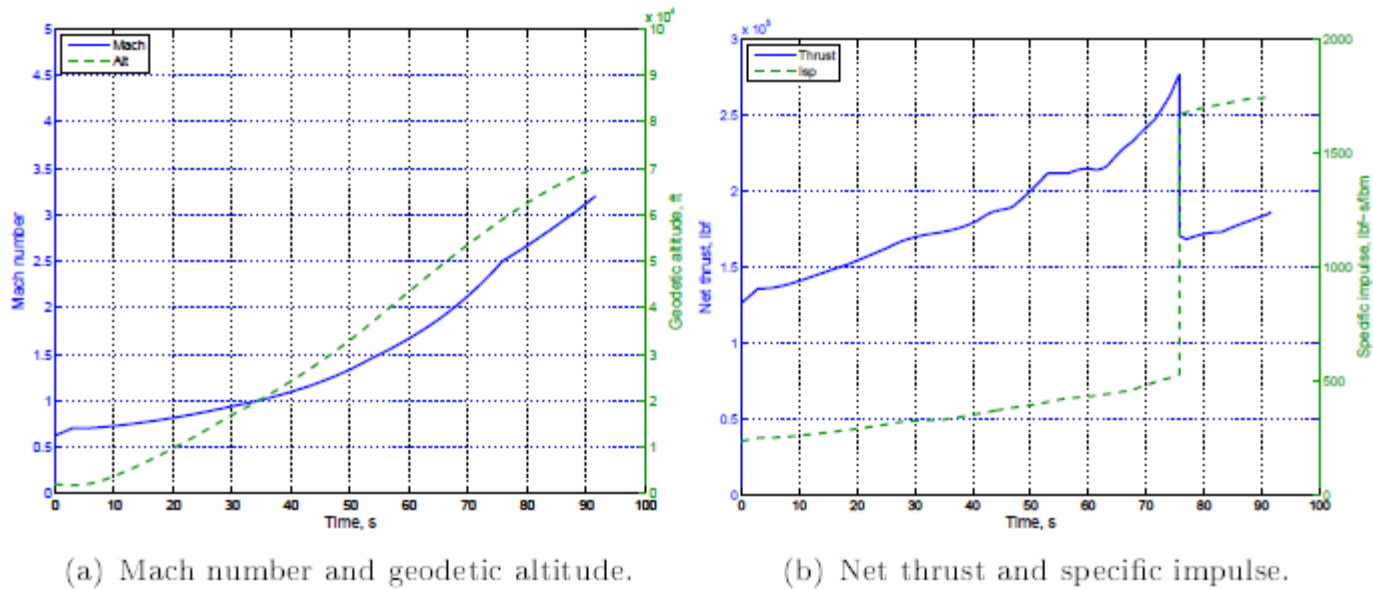


Figure 7. The simulated SR-71 ascent profile to Mach 3.2 and an altitude of 70,000 ft using the Marquardt MA139-XAA engine, with a staging point from ejector ramjet mode to pure ramjet mode at Mach 2.5 (approximately 76 s).



Rocket-Based Combined Cycle to Extended Launch Condition

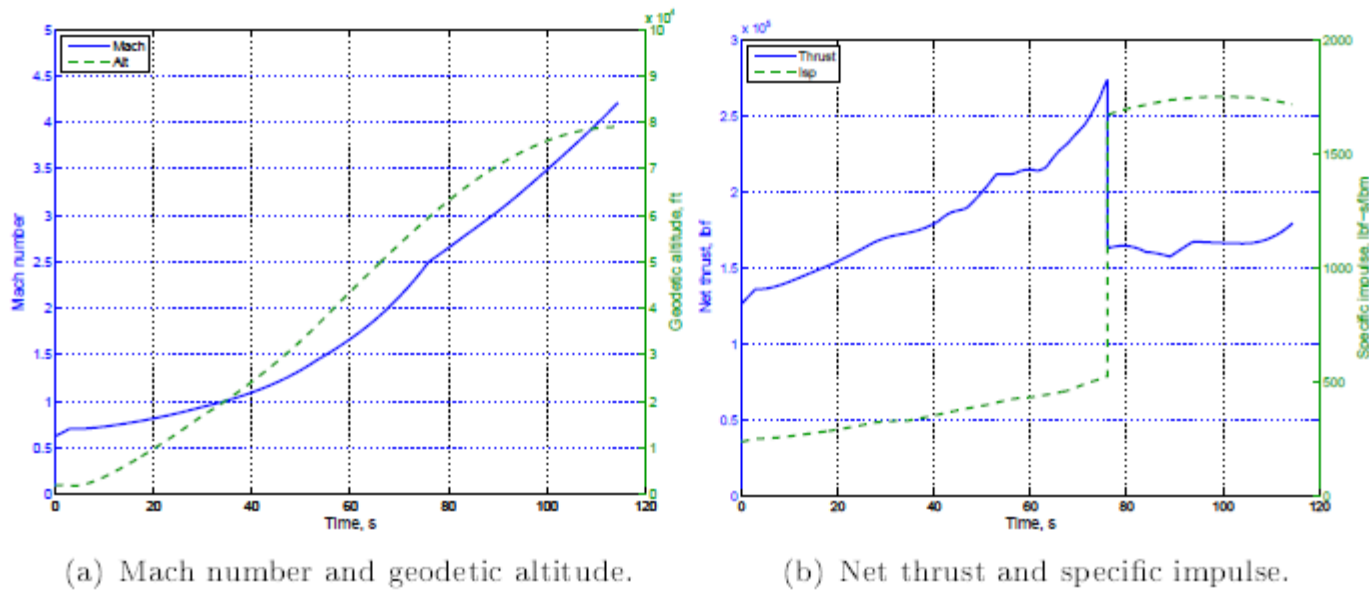


Figure 8. The simulated extended altitude and Mach number ascent profile to take advantage of the efficient, pure-ramjet-mode operation of the rocket-based combined-cycle engine.



Booster Staging / Separation Point

SR-71 + LASRE cruise condition

- Mach 3.0
- 70,000 ft

RBCC Extended Conditions

- Mach 4.5
- 80,000 ft



Solid Rocket Upper Stage Performance

Weight class, lbm	First-stage weight, lbm	First-stage thrust, lbf	Second-stage weight, lbm	Second-stage thrust, lbf	Payload to orbit, lbm
5000	4117	16650	711	2843	210
10000	8233	33300	1421	5686	432
15000	12350	49950	2132	8528	657
20000	16467	66500	2843	11371	882
25000	20583	83250	3553	14214	1095
30000	24700	99900	4264	17057	1330

Table 4. Payload delivered to a 100-nm circular orbit by a generic two-stage solid rocket system from a launch point of Mach 3.0 at an altitude of 70,000 ft.

Weight class, lbm	First-stage weight, lbm	First-stage, thrust, lbf	Second-stage weight, lbm	Second-stage thrust, lbf	Payload to orbit, lbm
Orion50XL+Star20					
10214	9551	34500	663	6100	355
Orion50XL+3XStar20s					
11540	9551	34500	1989	6100	524

Table 5. Payload delivered to a 100-nm circular orbit by a commercially-composed two-stage solid rocket system from a launch point of Mach 3.0 at an altitude 70,000 ft.



LOX/RP Upper Stage Performance

Weight class, lbm	First-stage weight, lbm	First-stage thrust, lbf	Second-stage weight, lbm	Second-stage thrust, lbf	Payload to orbit, lbm
5000	4116	16650	710	2843	243
10000	8350	33300	1196	4786	563
15000	12525	49950	1795	7179	844
20000	16700	66700	2293	9572	1133
25000	20875	83250	2991	11965	1421
30000	25050	99900	3589	14358	1711

Table 6. Payload delivered to a 100-nm circular orbit by a generic two-stage liquid-fueled rocket system from a launch point of Mach 3.0 at an altitude of 70,000 ft.

Weight class, lbm	First-stage weight, lbm	First-stage thrust, lbf	Second-stage weight, lbm	Second-stage thrust, lbf	Payload to orbit, lbm
10000	8350	33300	1196	4786	619
20000	16700	66700	2293	9572	1329
30000	25050	99900	3589	14358	2006

Table 7. Payload delivered to a 100-nm circular orbit by a generic two-stage liquid-fueled rocket system from the simulated rocket-based combined-cycle (RBCC) extended launch point of Mach 4.25 at an altitude of 80,000 ft, selected to take advantage of the extended Mach number capability of the RBCC.



ROM Equivalency

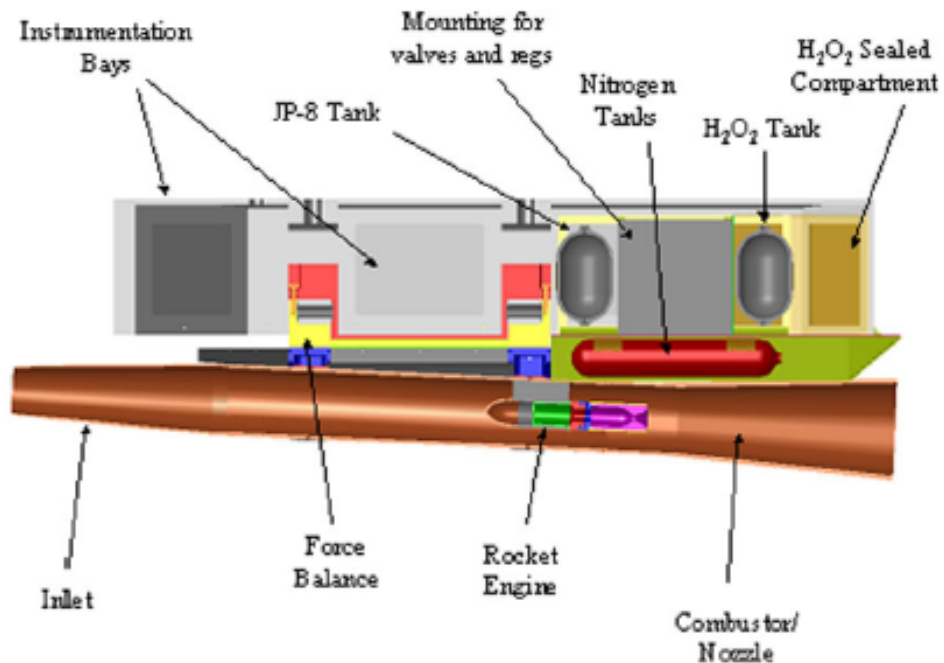
- SR-71 = 140000 lbs GLOW/ ~750 lbs LEO
- Falcon 1 = 61000 lbs GTOW/~750 lbs LEO

- Dry Weights:
 - SR-71 ~60,000 lbs + 2nd stage inert
 - Falcon 1 ~ 4520 lbs

- Future Studies:
 - What is the operational business case for a flyback booster?
 - Can a modern day Mach 3 booster system be designed for less than 60Klbs?



The Pathway to Flight-Testing Combined-Cycle Engines



The Ducted Rocket EXperiment, or D-REX. The D-REX project will explore flow dynamics related to ramjet ejector mode operation.

- Research will support the three further objectives of Joint Technology Office (JTO) on Hypersonics.
- ability to rapidly and accurately simulate variable-Mach airflow using variable geometric structures to constrict or expand the airflow in response to testing requirements
 - ability to rapidly and accurately simulate airflow transients to assess impact on aerodynamics and propulsion using variable geometric structures
 - ability to obtain in-stream measurements to assess combustion processes on a vehicle under test



Flight-Testing Combined-Cycle Engines



Figure 10. A NASA Dryden Flight Research Center F-15B shown in flight with the Rake Airflow Gage Experiment attached to the Propulsion Flight Test Fixture.

Combined Cycle Propulsion Work at NASA Dryden Flight Research Center:
NASA F-15B Propulsion Flight Test Fixture (PFTF)

- 2000 lbf six-degree-of-freedom instrumented force balance, in-flight measurement

Completed Rake Airflow Gage Experiment (RAGE)

- ascertain local flow Mach number and flow angularity underneath the F-15B

Proposed Channeled Centerbody Inlet Experiment (CCIE) FY2011

- Variable-geometry, mixed-compression inlet, explore the off-design performance & inlet distortion



Questions?

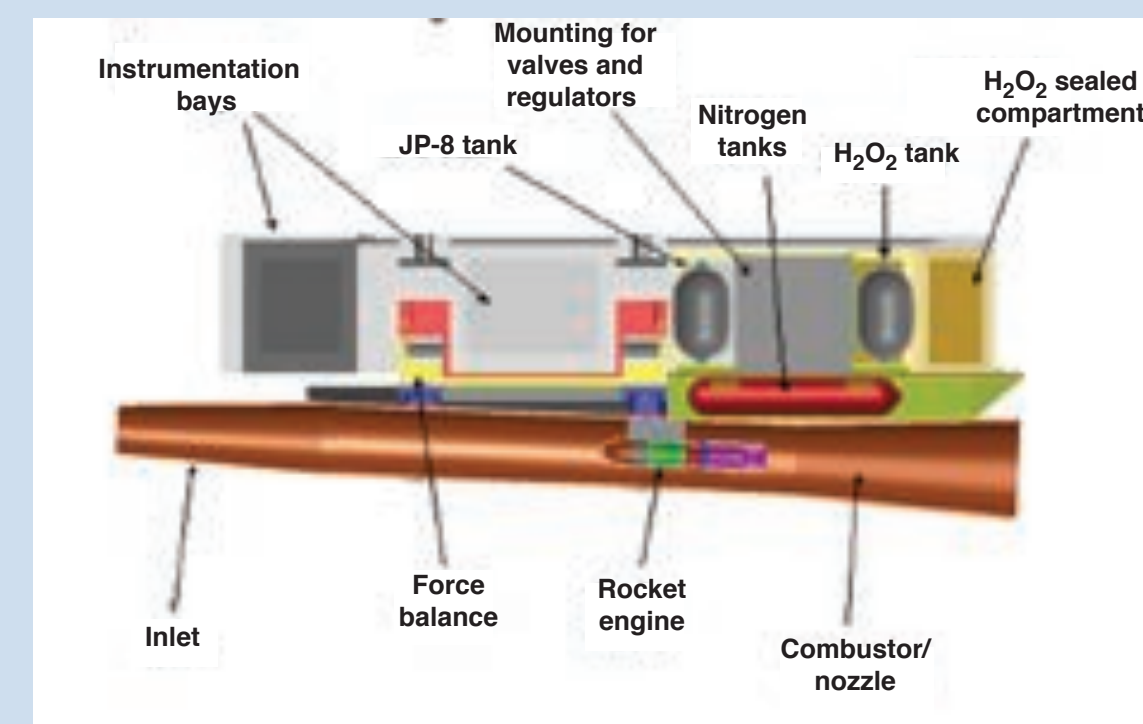
- Hugh L. Dryden – “...Separate the real from the imagined...”
- Modern day expression- “Flight is the only Truth!”
- Questions?

A Technology Pathway for Airbreathing, Combined-Cycle, Horizontal Space Launch Through SR-71 Based Trajectory Modeling

Kurt Kloesel, Nalin A. Ratnayake, and Casie M. Clark • NASA Dryden Flight Research Center, Edwards AFB, Edwards, CA

Analysis Objectives

- Examines the technical performance aspects of the commercialization of an air-breathing booster stage
- Performance comparison between air breathing booster system and LOX-RP all rocket system



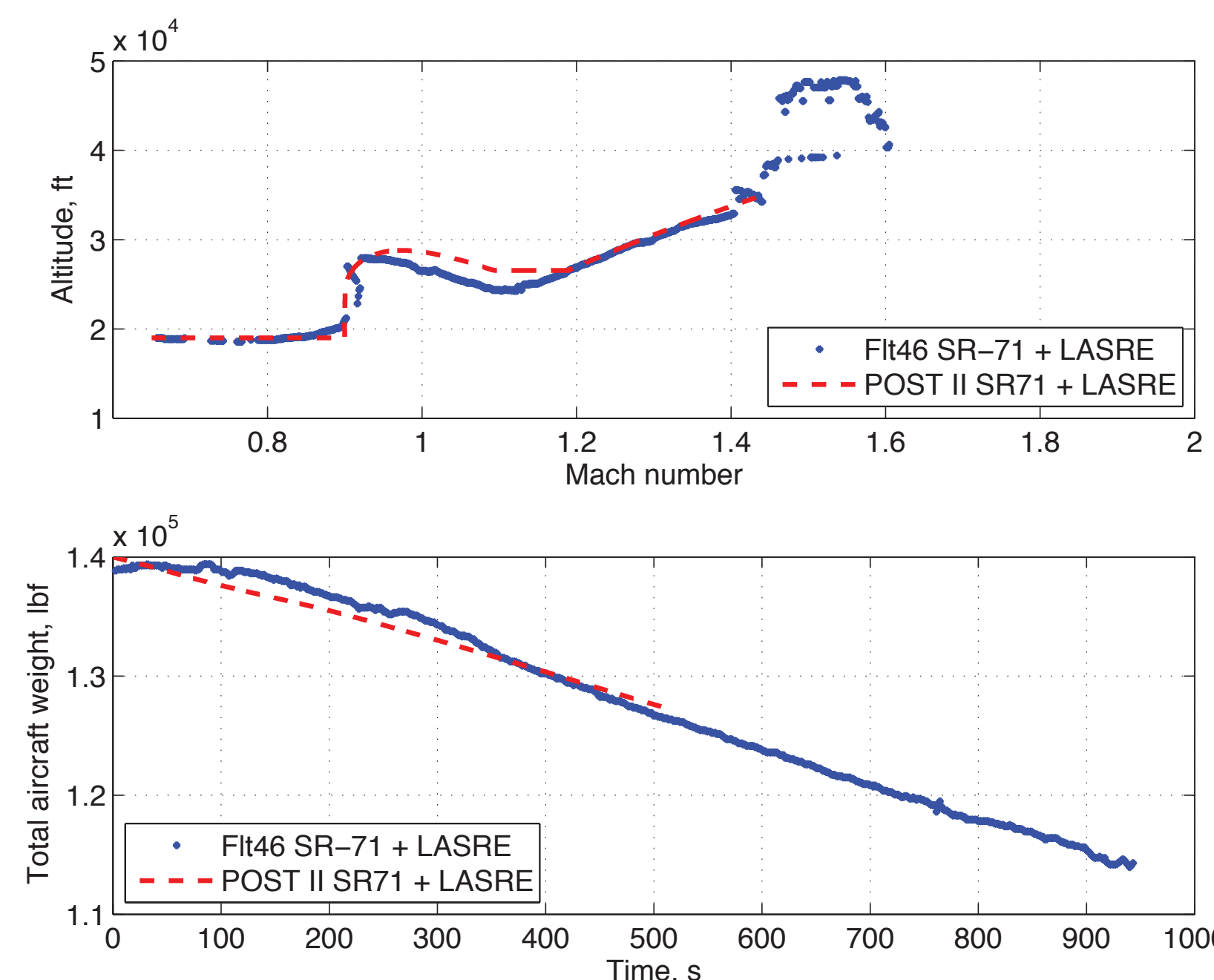
The Ducted Rocket Experiment, or D-REX. The D-REX project will flow dynamics related to ramjet ejector mode operation. Research will support the three further objectives of Joint Technology Office (JTO) on Hypersonics

- Ability to rapidly and accurately simulate variable-Mach airflow using variable geometric structures to constrict or expand the airflow in response to testing requirements
- Ability to rapidly and accurately simulate airflow transients to assess impact on aerodynamics and propulsion using variable geometric structures
- Ability to obtain in-stream measurements to assess combustion processes on a vehicle under test

The Lockheed SR-71 Blackbird in flight with the Linear Aerospike SR-71 Experiment (LASRE) attached.

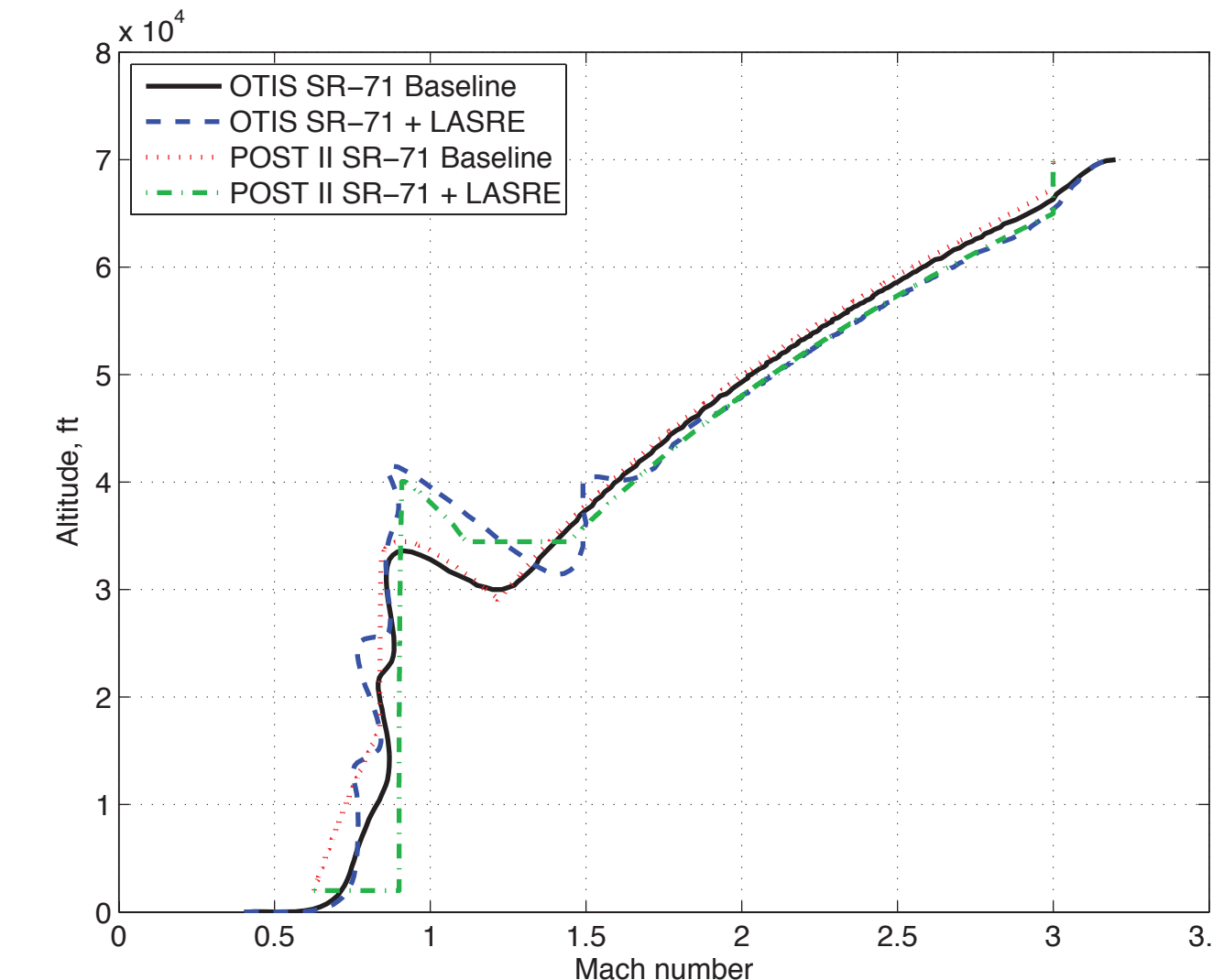
Combined Cycle Propulsion Work at NASA Dryden Flight Research Center:
 NASA F-15B Propulsion Flight Test Fixture (PFTF)
 • 2000 lbf six-degree-of-freedom instrumented force balance, in-flight measurement
 Completed Rake Airflow Gage Experiment (RAGE)
 • Ascertain local flow Mach number and flow angularity underneath the F-15B
 Proposed Channeled Centerbody Inlet Experiment (CCIE) FY2011
 • Variable-geometry, mixed-compression inlet, explore the off-design performance and inlet distortion

SR-71 + LASRE Model Performance Calibration



Aerodynamic model validation case in POST II compared to data from Flight 46 of the SR-71 with the LASRE.

SR-71 Performance Modeling

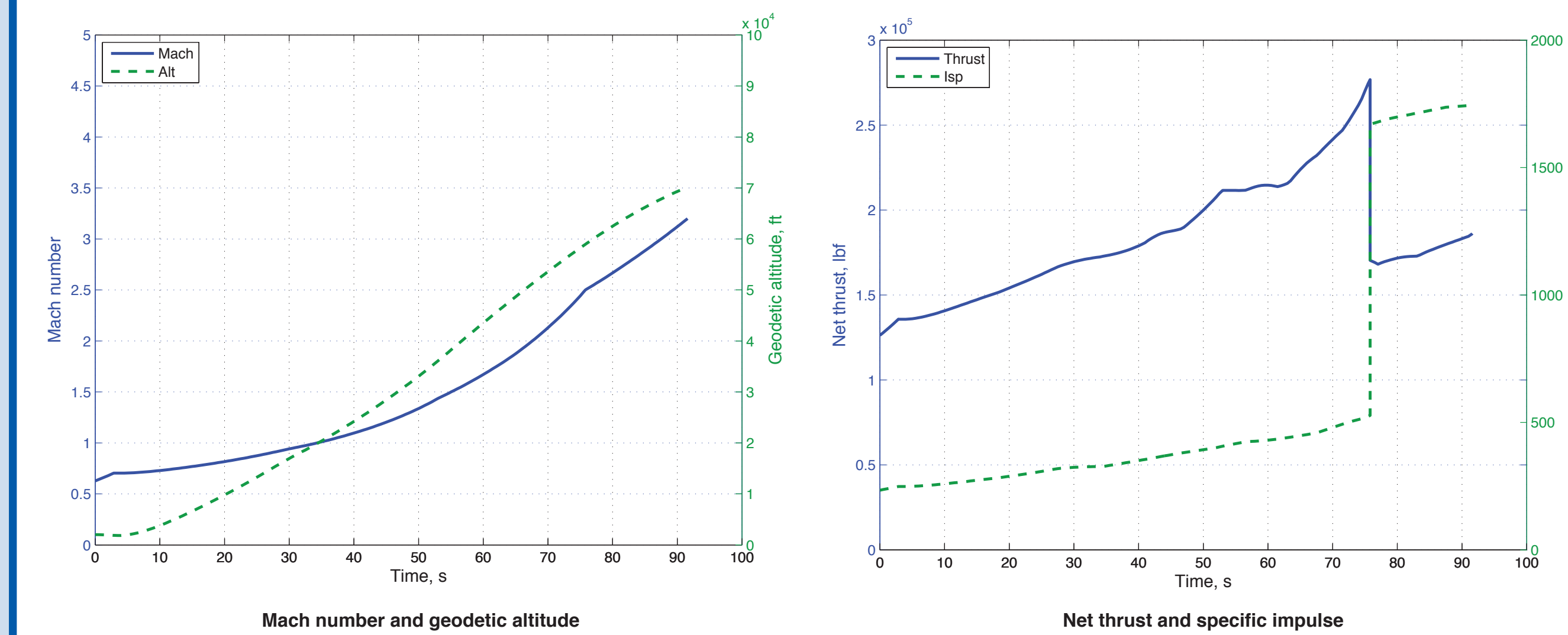


The OTIS (optimized) and POST II (piecewise non-optimized) minimum-energy climb profiles for the SR-71 and SR-71 + LASRE.

SR-71 configurations	Final weight, lbf	Total time, s	Final Mach number
OTIS baseline	119,120	1169	3.2
OTIS LASRE	113,348	1485	3.2
POST baseline	114,300	1631	3.0
POST LASRE	106,260	1627	3.0

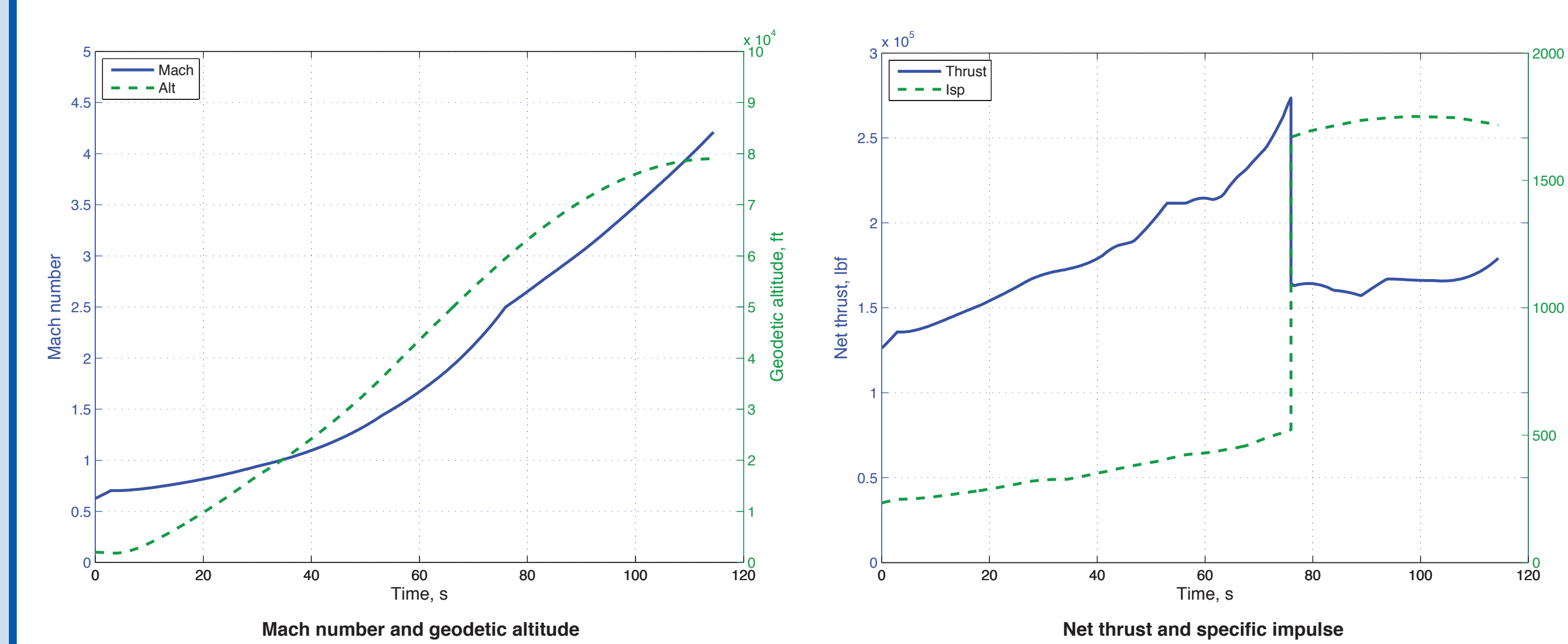
Results of OTIS and POST climb profiles indicating fuel consumption between the SR-71 baseline and the SR-71 LASRE

Rocket-Based Combined Cycle to SR-71 Cruise Condition



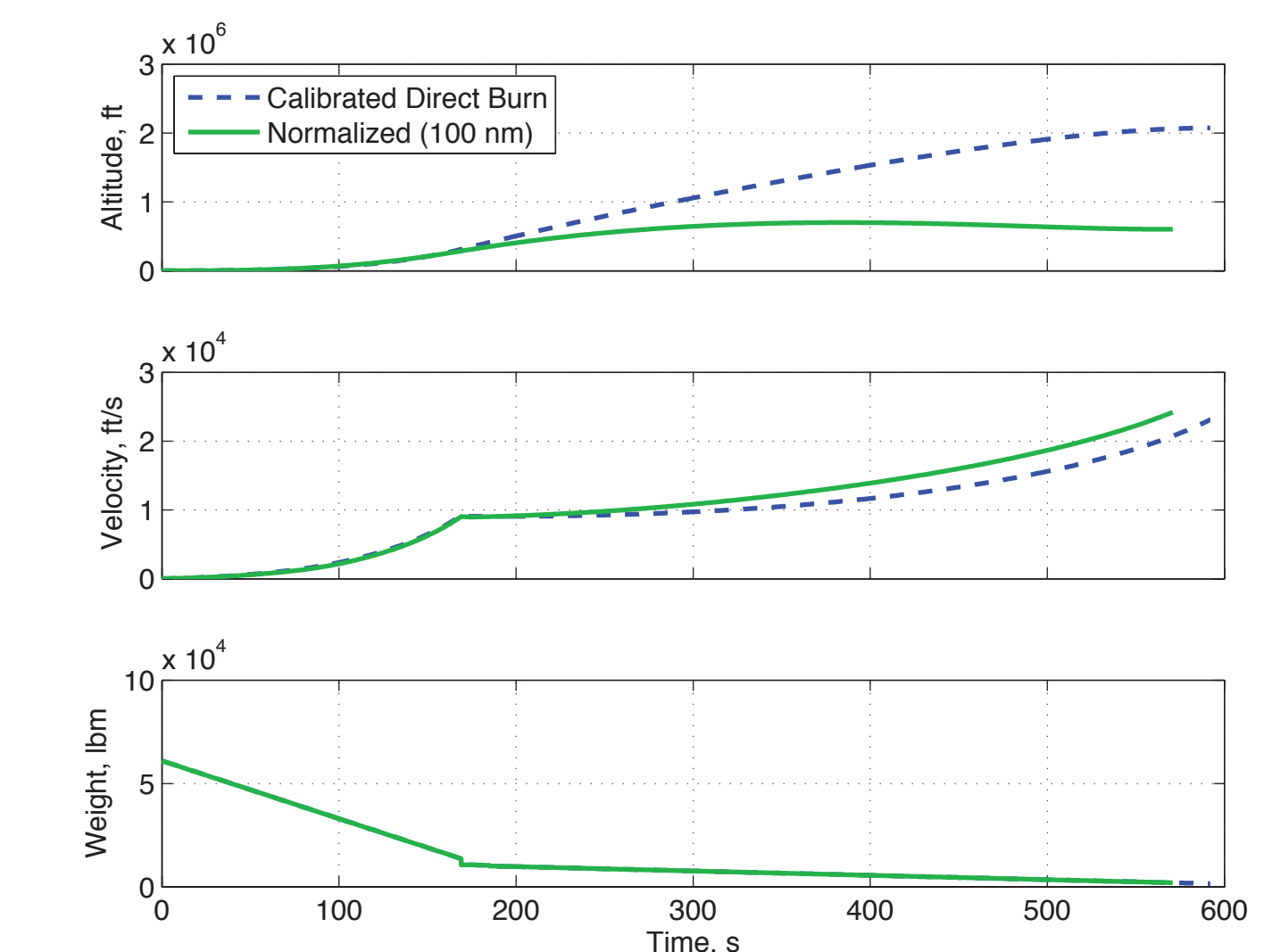
The simulated SR-71 ascent profile to Mach 3.2 and an altitude of 70,000 ft, using the Marquardt MA139-XAA engine, with a staging point from ejector ramjet mode to pure ramjet mode at Mach 2.5 (approximately 76 s).

Rocket-Based Combined Cycle to Extended Launch Condition



The simulated extended altitude and Mach number ascent profile to take advantage of the efficient, pure-ramjet-mode operation of the rocket-based combined-cycle engine.

Baseline LOX/RP All Rocket to LEO Performance



The geodetic altitude, velocity magnitude, and total launch vehicle weight compared with time for the simulated Falcon-1 ascent, shown for a calibrated direct burn and a normalized 100-nm circular orbit.

Solid Rocket Upper Stage Performance

Weight class, lbf	First-stage weight, lbf	First-stage thrust, lbf	Second-stage weight, lbf	Second-stage thrust, lbf	Payload to orbit, lbf
5000	4117	16650	711	2843	210
10000	8233	33300	1421	5686	432
15000	12350	49950	2132	8528	657
20000	16467	66500	2843	11371	882
25000	20583	83250	3553	14214	1095
30000	24700	99900	4264	17057	1330

Payload delivered to a 100-nm circular orbit by a generic two-stage solid rocket system from a launch point of Mach 3.0 at an altitude of 70,000 ft.

Weight class, lbf	First-stage weight, lbf	First-stage thrust, lbf	Second-stage weight, lbf	Second-stage thrust, lbf	Payload to orbit, lbf
Orion50XL - Star20	10214	9551	34500	663	355
Orion50XL - 3XStar20s	11540	9551	34500	1989	524

Payload delivered to a 100-nm circular orbit by a commercially-composed two-stage solid rocket system from a launch point of Mach 3.0 at an altitude of 70,000 ft.

LOX/RP Upper Stage Performance

Weight class, lbf	First-stage weight, lbf	First-stage thrust, lbf	Second-stage weight, lbf	Second-stage thrust, lbf	Payload to orbit, lbf
5000	4116	16650	710	2843	243
10000	8230	33300	1396	4786	363
15000	12325	49950	1795	7179	544
20000	16700	66700	2293	9572	813
25000	20875	83250	2991	11965	1021
30000	25050	99900	3589	14358	1211

Payload delivered to a 100-nm circular orbit by a generic two-stage liquid-fueled rocket system from a launch point of Mach 3.0 at an altitude of 70,000 ft.

Weight class, lbf	First-stage weight, lbf	First-stage thrust, lbf	Second-stage weight, lbf	Second-stage thrust, lbf	Payload to orbit, lbf
10000	8250	33300	1196	4786	619
20000	16700	66700	2293	9572	1329
30000	25050	99900	3589	14358	2086

Payload delivered to a 100-nm circular orbit by a generic two-stage liquid-fueled rocket system from the simulated rocket-based combined-cycle (RBCC) extended launch point of Mach 4.25 at an altitude of 80,000 ft, selected to take advantage of the extended Mach number capability of the RBCC.

Turbojets: 50 years of improvements

J-58/JT11D-20A Performance*

- 32,000 lbf of afterburning thrust at STP
- Dry weight of 6,000 lb
- Thrust-to-weight ratio of 5.3:1



F100-PW-229 Performance*

- 29,160 lbf of afterburning thrust at STP
- Dry weight of 3,740 lb
- Thrust-to-weight ratio of 7.8:1

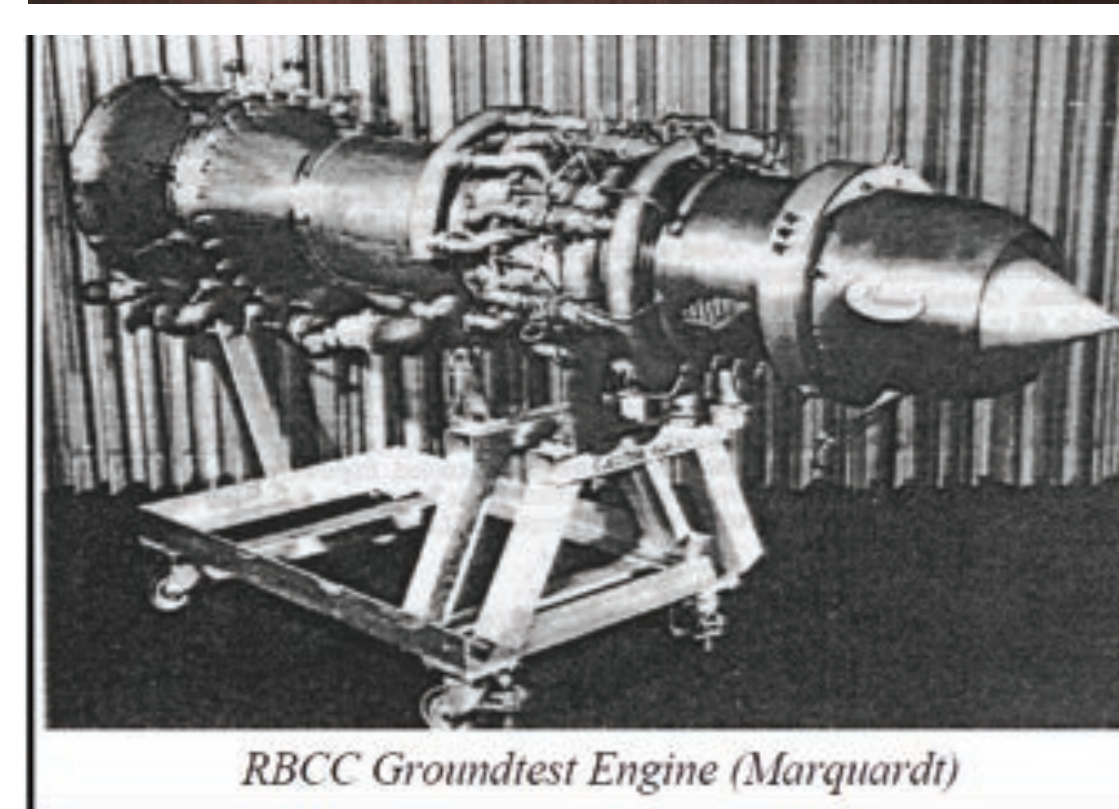


*These numbers represent the core attributes of both engines and do not include the weight of variable-inlet machinery for either engine or the ejector nozzle on the J-58.

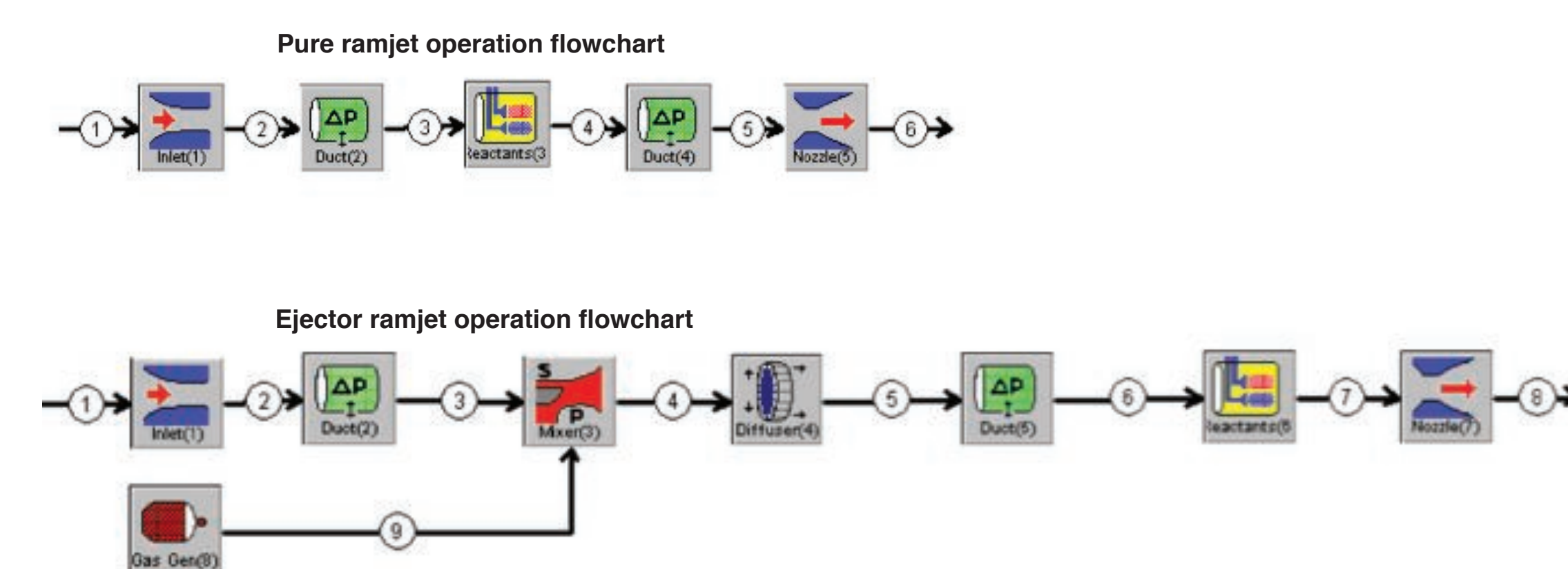
RBCC Performance

MA139-XAA engine, Ejector ramjet 80,000 lbf @ STP liquid oxygen and rocket propellant (LOX/RP) primary (rocket) combustors, hydrocarbon fuel afterburner

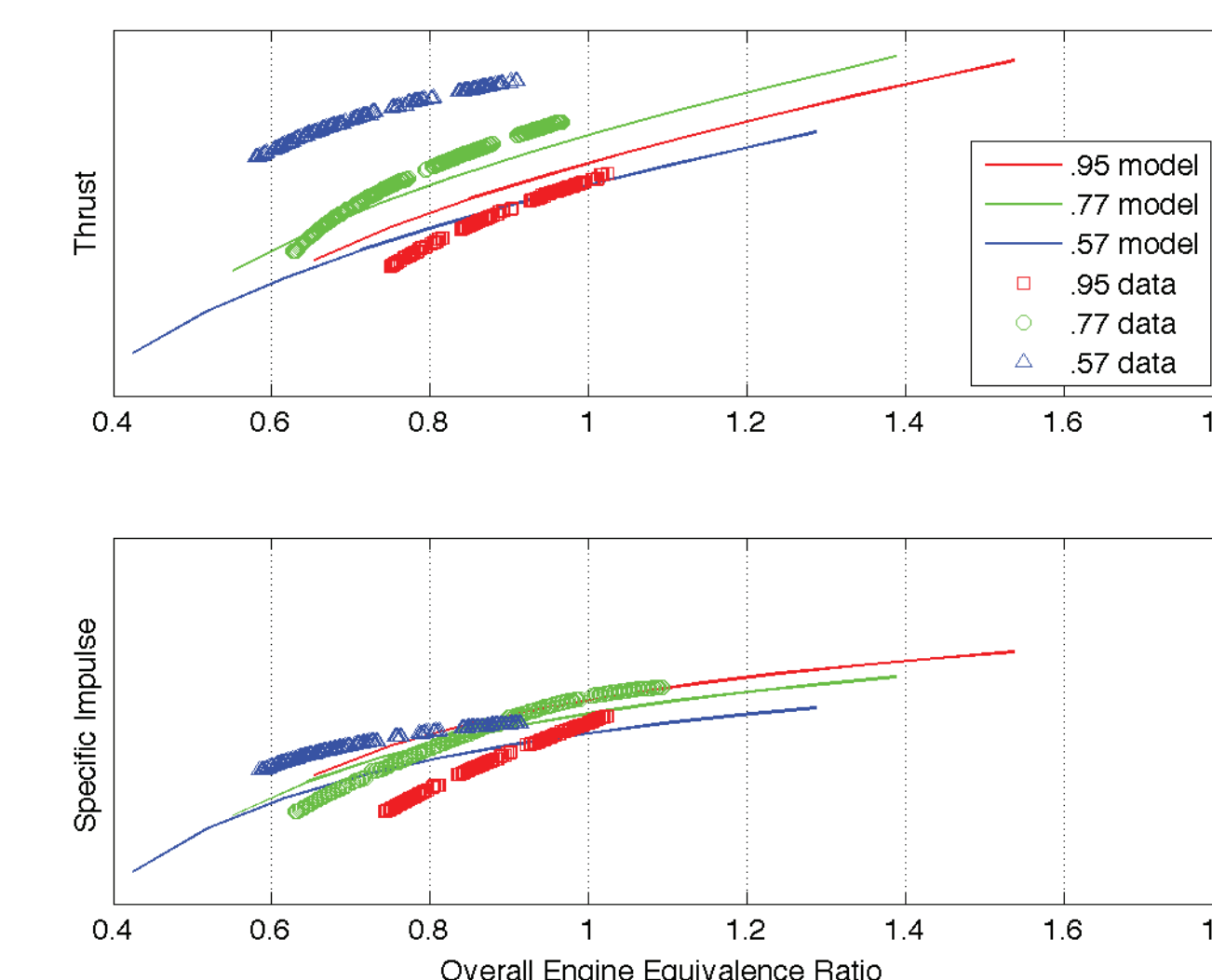
A cluster of 24 regeneratively-cooled LOX/RP rockets forms the primary system, each with 2,960 lbf of thrust at standard conditions. Hydrocarbon injectors are used for the afterburner, which is downstream of the mixing chamber. Each engine weighs 5,300 lbf and generates 80,000 lbf of sea level static thrust (where augmentation is least effective). Ground-test data are available for a number of different equivalence ratios, secondary-to-primary flow ratios, mixer inlet Mach numbers, and flight Mach numbers, each for various propellant combinations. The engine data used in the present study were for primary chamber pressure of 600 psia, the primary and afterburner combustion chambers at stoichiometric equivalence ratio, and primary and afterburner chambers operating at 0.95 efficiency.



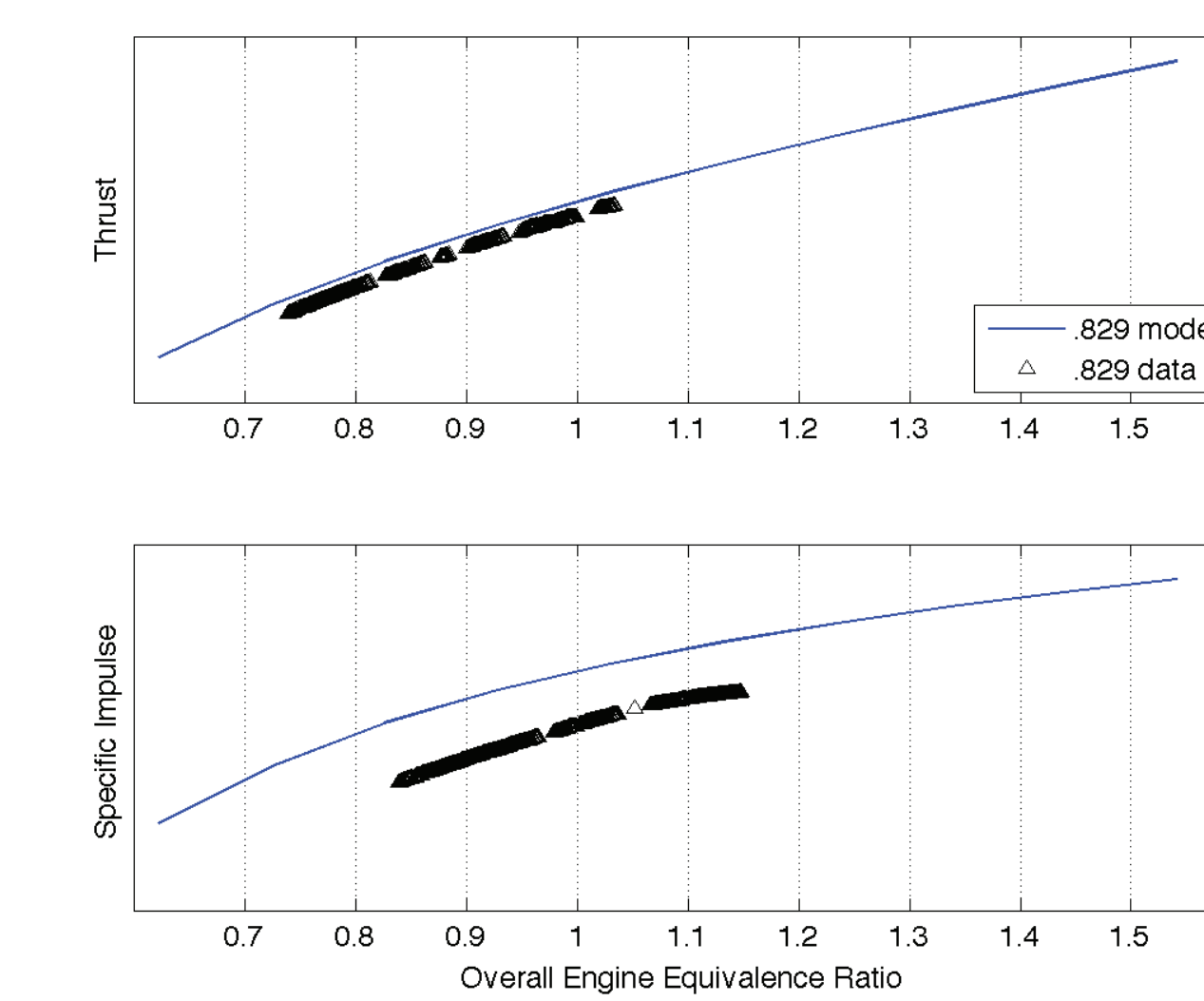
GE-CAT Ejector Ramjet Engine Modeling



Flowchart of the Graphical Engine Cycle Analysis Tool model for the subscale Marquardt Corp. ejector ramjet



The Graphical Engine Cycle Analysis Tool rocket-based combined-cycle model estimates of sea level static thrust and specific impulse compared with the overall engine equivalence ratio, plotted against Marquardt Corp. test data.



The Graphical Engine Cycle Analysis Tool rocket-based combined-cycle model estimates of sea level static thrust and specific impulse compared with the overall engine equivalence ratio, plotted against Marquardt Corp. test data.

Model error	Net thrust, percent	I _{sp} , percent
Static $\Phi_p = 0.95$	4.89	6.48
Static $\Phi_p = 0.77$	2.46	2.07
Static $\Phi_p = 0.57$	19.94	4.52
Mach 1.9 (ejector), $\Phi_p = 0.829$	2.09	6.58
Mach 1.9 (ramjet), $\Phi_p = 0.829$	5.25	8.47

Average error versus Marquardt Corp. engine data for the Graphical Engine Cycle Analysis Tool rocket-based combined-cycle model at certain Mach numbers, configurations, and primary (rocket) equivalence ratios.